FRONTIERS OF PHYSICS

TOPICAL REVIEW
Volume 18 / Issue 2 / 21303 / 2023

Rare-earth quantum memories: The experimental status quo

Mucheng Guo[1,2], Shuping Liu[1,2,3], Weiye Sun[1,2], Miaomiao Ren[1,2], Fudong Wang[1,2,3,†], Manjin Zhong[1,2,3,‡]

1 Shenzhen Institute for Quantum Science and Engineering, Southern University of Science and Technology, Shenzhen 518055, China
2 International Quantum Academy, Shenzhen 518048, China
3 Guangdong Provincial Key Laboratory of Quantum Science and Engineering, Southern University of Science and Technology, Shenzhen 518055, China
Corresponding authors. E-mail: †wangfd@sustech.edu.cn, ‡zhongmj@sustech.edu.cn
Received November 10, 2022; accepted December 2, 2022

ABSTRACT

Rare-earth doped crystals carry great prospect in developing ensemble-based solid state quantum memories for remote quantum communication and fast quantum processing applications. In recent years, with this system, remarkable quantum storage performances have been realized, and more exciting applications have been exploited, while the technical challenges are also significant. In this paper, we outlined the status quo in the development of rare-earth-based quantum memories from the point of view of different storage protocols, with a focus on the experimental demonstrations. We also analyzed the challenges and provided feasible solutions.

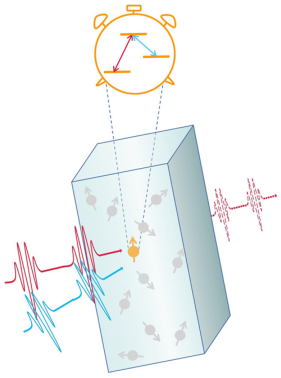

Keywords solid-state quantum memory, rare-earth crystals, quantum network, quantum communication

Contents

*Special Topic: Embracing the Quantum Era: Celebrating the 5th Anniversary of Shenzhen Institute for Quantum Science and Engineering (Eds.: Dapeng Yu, Dawei Lu & Zhimin Liao).

1 Introduction

Based on the fundamental principles of quantum mechanics, quantum information science provides people with a brand-new way of information acquisition, processing and transmission [1–6]. One of the ultimate goals of modern quantum information science is to build a global quantum network that is analogous to the internet we are using nowadays [7–9]. The basic element of such

Higher Education Press

https://doi.org/10.1007/s11467-022-1240-8

a quantum network is a quantum computer in which entangled quantum states are used to perform computations in parallel, allowing some computation tasks to be dramatically more efficient than conventional computers. A quantum network is then realized through interconnecting quantum computers by using particles to distribute entanglement [10].

Among the many material systems, photons are considered the natural information carrier in the quantum network because it is easier to generate and transmit. However, the direct transmission range of light is limited by losses associated with scattering, diffraction, and absorption in optical fibers [11–13]. Restrained by the non-cloning theorem, direct amplification of quantum states encoded on the optical modes is not possible [14]. A feasible solution to overcome this range limitation is the quantum repeater proposal, which involves dividing a distant link to many nodes and distributing entangled photon pairs between these nodes [15–18]. Instead of establishing entanglement simultaneously in all elementary links, quantum memories are stationed at each node such that entanglement can be stored and distributed gradually. Further, for practical quantum computer devices, the gate executions are carried out sequentially, and sometimes the calculation results need to be stored for later computation. Moreover, a viable strategy to synchronize operations is to create a gate execution delay for a qubit. Thus, implementing a quantum memory in a quantum computer system can afford more flexibility to perform processing tasks and sometimes can also reduce the number of required qubits [19–22].

There is significant interest in developing suitable memories based on mapping optical quantum states in the energy levels of a material system, while a significant milestone is the so-called DLCZ protocol (proposed by Duan, Lukin, Cirac & Zoller) [23]. It demonstrated for the first time the fundamental operation of a quantum repeater by integrating atomic ensemble and linear optical techniques [23]. In this proposal, on-demand conversion between the flying qubits encoded in photons and the stationary qubits in atomic ensembles can be conducted with high efficiency. This inspired vast research interest in quantum storage applications based on atomic ensembles, and many impressive experimental advances have been reported in recent years [24–43].

The atomic systems are used for developing quantum memories because states of their internal electronic levels are mostly well characterized and usually coupled weakly to the environment. In contrast, solid-state systems have strong interactions with the dynamic environment which results in short coherence times for their optical or hyperfine transitions, accordingly short quantum storage time. However, there is a unique solid-state system, rare-earth-ion (RE) doped crystals, which can possess long coherence time for both optical and hyperfine

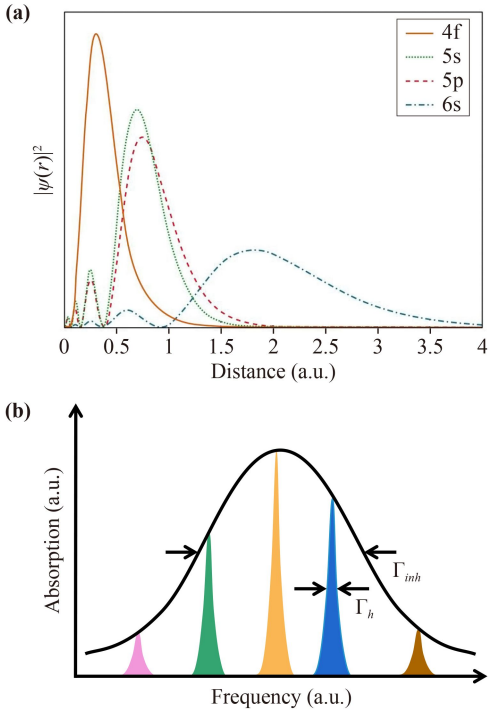

Fig. 1 **(a)** Radial for the 4f, 5s, 5p and 6s electrons of Gd^{+} [50]. **(b)** The inhomogeneous broadening Γ_{inh} arises since individual ion in the solid experiences a different static local environment. These differences lead to the respective optical transition frequency of each ion. The homogeneous broadening Γ_h is due to dynamical perturbations on the optical transition frequencies. And Γ_{inh} can be seen as the sum of the homogeneous broadening Γ_h of each ion within the ensemble.

transitions [44–47]. In this system, electrons of the optically addressable $4f^N$ levels are considered to have free-atom-like properties because they are well shielded by the full-filled outer electronic shells from interacting with the crystal environment [see Fig. 1(a)] [48, 49]. Secondly, the large ratio between inhomogeneous [see Fig. 1(b)] and homogeneous linewidth of RE crystals provides tremendous potential for multi-mode storage capacity. Further, as solid, RE crystals provide advantages from the point of view of engineering feasibility. Thus, this system is one of the most promising candidate for developing quantum storage devices and progress in storage performance based on different protocols has been achieved during the past decades.

In this paper, we aim to review the research progress of quantum-memory development based on RE crystals. The paper is arranged in the following way: in Section 2, we will introduce the basic performance criteria that a quantum memory needs to satisfy in the application of a quantum network. Section 3 and Section 4 introduce the main progress of absorptive quantum memories, including memories based on electromagnetically induced transparency (EIT) and photon-echo protocols. Finally, we finish the paper with a conclusion and outlook.

2 Quantum memory performance

In this section, we will discuss the main performance evaluation criteria concerned with the realization of a quantum memory, such as storage fidelity, storage time, storage efficiency, storage mode capacity and storage bandwidth.

To ensure the validity of the information in the stored procedure, (conditional fidelity) fidelity F is defined as the overlap between the density matrices ρ_{in} of the input state and ρ_{out}, the density matrices of the retrieved state, corresponding to the following equation:

$$F = (Tr\sqrt{\sqrt{\rho_{in}}\rho_{out}\sqrt{\rho_{in}}})^2. \quad (1)$$

The fidelity of the ideal stored procedure can reach the maximum value of 1 while in practical experiments, it is often required to exceed 2/3 for a classical memory [51, 52].

In general cases, the storage time is required to be comparable to the time for establishing the entanglement over the entire repeater link [16]. However, when quantum storage was applied to realize synchronization in the high-speed optical quantum network, the requirement for storage time is relatively flexible.

Storage efficiency is defined as the ratio between the energy of the retrieved signal and that of the input signal, which means the probability of re-emitting a photon. Improving storage efficiency can greatly increase the rate of entanglement distribution. For every 1% increase in storage efficiency, the entanglement distribution rate can increase about 10% [16].

Multi-mode storage can also increase the entanglement distribution rate while significantly reducing the stability requirements of the repeater protocol [53, 54]. Storage bandwidth is defined as the maximum frequency bandwidth of the optical signal that can be effectively stored. With the storage bandwidth δ and storage time τ, the dimensionless time bandwidth product is defined as $B = \delta \times \tau$ [55]. The maximum number of effective procedures can be stored within a fixed storage time determines the memory's synchronization capability.

Optical quantum memory is an indispensable part of many applications of quantum information [20]. However, each application has its specific requirements for the performance of the memory, which needs to be optimized according to the actual situation. For example, a memory used to buffer qubits in an optical quantum processor, due to the fast operations, may not require as long storage time as that in long-distance quantum communication, but it may concerns a lot about the bandwidth and multi-mode capacity.

3 EIT memories

In the DLCZ protocol, the material system work not only as a quantum memory but also as source of quantum states. In contrast, so-called absorptive memories work through converting quantum information encoded in light to atomic excitations of a material system, storing and retrieving the quantum information on demand. Historically, absorptive quantum memories developed along two distinct paths, that are optically controlled memories and photon echo memories [56]. In an optically controlled memory, intense control pulses are used to activate absorption and retrieval, two typical examples of which are the Raman memory and the EIT protocol [57–59]. The main difference is that the control field is off-resonant for the Raman scheme and on-resonance for the EIT protocol. To be effective, high excitation rate is required for the off-resonance Raman process while in RE solids, oscillation strength of transitions is usually very weak because they are parity forbidden, thus this protocol has not received that much attention [50]. Hence, in this section, we will introduce the EIT scheme as an example of optically controlled memories. The name EIT was first termed by Harris and his co-workers at Stanford University in 1990 [59] and has been continuously active in the research work on quantum storage.

3.1 EIT slow light

In a three-level of lambda configuration shown in Fig. 2(a), the transition between the two lower energy states, $|g\rangle$ and $|s\rangle$, is dipole-forbidden while transitions of both states to an excited state, $|e\rangle$, is allowed. We call a beam that couples $|g\rangle$ and $|e\rangle$ the "signal" beam and a beam that couples $|s\rangle$ and $|e\rangle$ the "control" beam. Both beams can be absorbed by the atoms if they enter the atomic medium alone. However, when the two beams are applied simultaneously, they interfere destructively, which can cause a transparency window in the signal field if the control beam is strong. The response of the atomic ensemble to the input beams can be described in terms of the susceptibility X [60–62]:

$$X \approx X_R + \mathrm{i}X_I, \quad (2)$$

$$X_R = 4\frac{N}{V}\frac{|\mu_{ge}|^2}{\epsilon_0\hbar}\frac{-\delta(|\Omega_c|^2 - 4\Delta_s\delta) + \Delta_s\Gamma_s^2}{|(\Gamma_e + \mathrm{i}2\Delta_s)(\Gamma_s + \mathrm{i}2\delta) + |\Omega_c|^2|^2}, \quad (3)$$

$$X_I = 2\frac{N}{V}\frac{|\mu_{ge}|^2}{\epsilon_0\hbar}\frac{\Gamma_s(|\Omega_c|^2 + \Gamma_s\Gamma_e) + 4\delta^2\Gamma_e}{|(\Gamma_e + \mathrm{i}2\Delta_s)(\Gamma_e + \mathrm{i}2\delta) + |\Omega_c|^2|^2}, \quad (4)$$

where $\Delta_s = w_{eg} - w_s$, $\Delta_c = w_{es} - w_c$ are detuning of the signal beam the control beam while $\delta = \Delta_s - \Delta_c$ is the two photon detuning. Also, Γ_e and Γ_s are the decoherence rates of the $|e\rangle \to |g\rangle$ and $|s\rangle \to |g\rangle$ transitions respectively, N is the total number of atoms in the sample, and Ω_s and Ω_c are the Rabi frequency for the signal and the control field.

In a situation when $\delta = 0$, that is $\Delta_s = \Delta_c = \Delta$, an

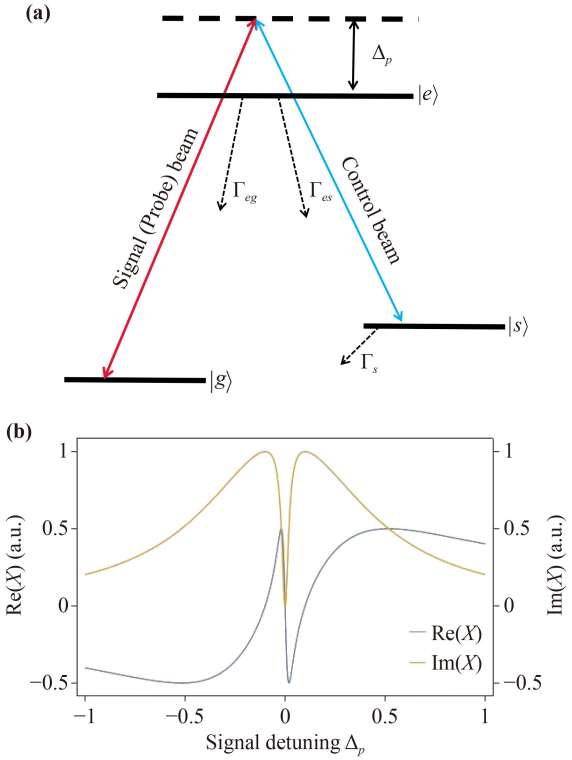

Fig. 2 **(a)** Three-level system in Λ configuration. The signal (probe) beam and control beam drive the transition $|g\rangle \leftrightarrow |e\rangle$, $|s\rangle \leftrightarrow |e\rangle$ respectively. The transition between the two lower energy states ($|g\rangle \leftrightarrow |s\rangle$) is dipole-forbidden and atoms can stay in either of the two states for a long time. $\Gamma_e = \Gamma_{es} + \Gamma_{eg}$ and Γ_s corresponding to the decoherence rate. **(b)** Under the ideal condition of $\Gamma_s = 0$, $\Delta_c = 0$, the linear susceptibility X for the signal optical field as the function of the single photon detuning Δ_p. The imaginary part of X [Im(X)] indicates the existence of a transparent window at the single-photon resonance, and simultaneously its real part [Re(X)] means that the signal light has a strong dispersion in the medium.

ideal EIT medium, for which the relaxation rate between the two lower energy states, $|g\rangle$ and $|s\rangle$, is very small, i.e., $\Gamma_s \to 0$ and $X \approx 0$ accordingly, we will have Eq. (4) to describe the system. In this equation, X_I determines the dissipation of the field by the ensemble, i.e., absorption coefficient α, while X_R determines the refractive index n of the EIT medium. This indicates that there is neither dispersion nor absorption in the medium, which corresponds to the electromagnetic induction transparency (EIT) phenomenon,

$$n = \mathrm{Re}\sqrt{1+X} \approx 1 + \frac{1}{2}X_R,$$
$$\alpha = \frac{4\pi}{\lambda}\mathrm{Im}\sqrt{1+X} \approx \frac{2\pi}{\lambda}X_I, \tag{5}$$

According to Eq. (4), the linear susceptibility spectrum of an EIT medium can be drawn as Fig. 2(b). In a narrow transparent windows, the refractive index changes steeply, which causes the group velocity ν_g of the signal light to be less than the speed of light traveling in vacuum [see Fig. 2(a)], and in the meantime, the medium's absorption can be significantly reduced. This is the so-called slow light effect.

In RE crystals, Ham *et al.* [63] reported transmission without absorption in a Y^{3+} doped Y_2SiO_5 (YSO) crystal at temperature of 5 K for the first time. In this work, $|g\rangle$ and $|s\rangle$ are hyperfine states of $^3H_4$, $|e\rangle$ is $^1D_2$. Wavelengths of signal and control beams are about 605.7 nm, splittings of $|g\rangle$ and $|s\rangle$ is about tens of MHz. After this pioneering work, light speeds of 45 m/s and even stopping of the light were also observed in the same system [64–66]. These successful EIT demonstrations inspired vast research interests in conducting EIT quantum storage in RE crystals.

3.2 EIT storage

The EIT storage process can be described by the Bloch–Maxwell equations [57], in which the time-dependent spin wave $S_{sg}(z,t)$ is mapped from polarization $P_{eg}(z,t)$ and signal field $\mathcal{E}_{in}(z,t)$ under the control beam $\Omega_c^*(t-z/c)$,

$$\begin{aligned}(\partial_t + c\partial_z)\,\mathcal{E}_{in}(z,t) &= \mathrm{i}g\sqrt{N}P_{eg}(z,t),\\ \partial_t P_{eg}(z,t) &= -(\gamma+\mathrm{i}\Delta)P_{eg}(z,t)+\mathrm{i}g\sqrt{N}\mathcal{E}_{in}(z,t)\\ &\quad + \mathrm{i}\Omega_c(t-z/c)S_{sg}(z,t),\\ \partial_t S_{sg}(z,t) &= \mathrm{i}\Omega_c^*(t-z/c)P_{eg}(z,t).\end{aligned} \tag{6}$$

For optimal efficiency, the system should be controlled in a time-reversal procedure. The phase matching requires $k_{in} - k_{w,c} = k_{out} - k_{r,c}$, where the four terms are wave vectors of input pulse, control write pulse, output pulse and control read pulse, respectively. Thus, the maximum storage efficiency of a forward readout is slightly lower than a backward retrieval readout because it does not correspond to a complete reversal of the write procedure [58].

In the EIT process, the group velocity of the signal field is so low that the entire pulse is compressed and stored in the sample. Meanwhile, in order to avoid absorption, the spectral bandwidth of the signal pulse must be narrower than the EIT window Γ_{EIT}. This suggests that the signal pulse shape must fulfill a compromise between spectral and spatial conditions for efficient storage, which can be written as [69, 72]

$$\Gamma_{EIT} \approx \frac{\Omega_c^2\sqrt{\ln 2}}{\Gamma_e\sqrt{\alpha L}} \gg \frac{1}{\tau_s} \iff \frac{\Omega_c^2\tau_s}{\Gamma_e} \gg \sqrt{d},$$
$$L \geq v_g\tau_s \approx \frac{\Omega_c^2\tau_s}{\alpha\Gamma_e} \iff d \geq \frac{\Omega_c^2\tau_s}{\Gamma_e}. \tag{7}$$

In this equation, d is the optical depth, Ω_c is control Rabi frequency and τ_s is the signal pulse duration. The equation implies that high optical depth of a medium is

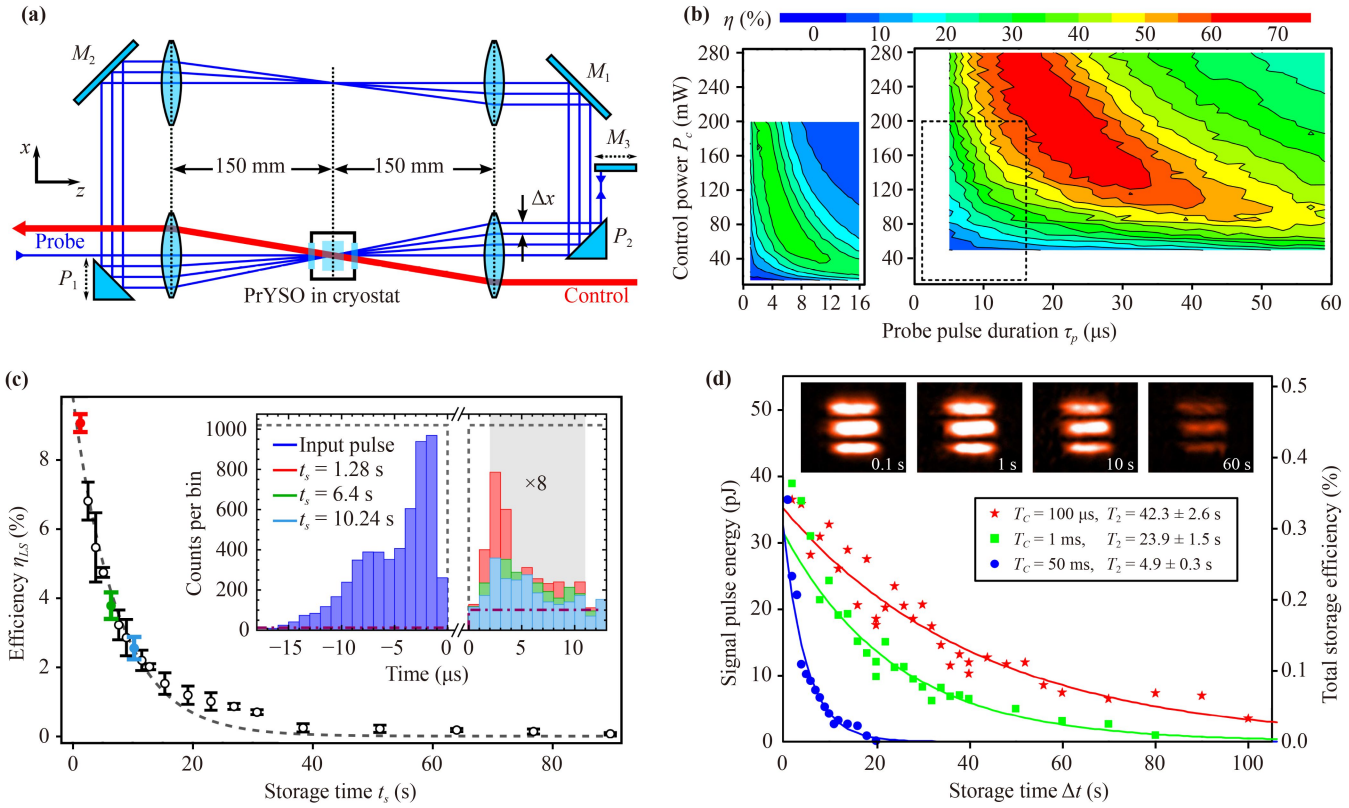

Fig. 3 Experimental demonstration of EIT storage in RE systems. **(a)** Schematic of multi-pass configuration. The number of round-trips be adjusted by the movable mirror M_3 in z direction [69]. **(b)** Experimental result of EIT storage efficiency η with control power P_c and probe pulse duration τ_p [69]. Left: $N_{pass} = 1$; Right: $N_{pass} = 10$. The parameter range in the dotted box correspond to the left figure [69]. **(c)** Experimental results showing optical storage efficiency η_{LS} decay with storage time t_s for $\overline{n} = 52 \pm 2$. Inset: Photon counts of the input pulse (blue) and signal pulses at different storage times of $t_s = 1.28$ s (red), 6.4 s (green), and 10.24 s (cyan) [70]. **(d)** Output image energy intensity as a function of storage time Δt. The three data sets correspond to different cycling times in the dynamical decoupling sequence. The insets show the results of image storage and retrieval in the setup [71].

required for EIT-based memories to achieve high storage efficiency. In cold atoms, a feasible solution is to increase the dimension of a magneto-optical trap (MOT) [73, 74], which leads to impressive storage efficiency, 92.0% for a coherent optical memory [75], quantum memory for single-photon polarization qubits with an efficiency of more than 85% [76]. One of the primary concerns with this system is the diffusion of atoms, imposing a limit on the longest achievable storage time.

For RE crystals based memory, a low concentration of RE ions are trapped in crystal lattice, so the atomic diffusion is not a concern but the low optical depth is still a challenge. The first report of EIT storage in RE crystal is performed in Pr^{3+}:YSO, with a storage time longer than 1 second. However, the overall storage efficiency is only 1% due to the low optical density. This is because the relevant transitions are within the $4f^N$ shell which are parity forbidden but only become weakly allowed as a result of the level mixing caused by the crystal field.

A feasible way to achieve higher optical depth is to extend the light path in the medium. To avoid causing more inhomogeneity in the control field from a longer crystal, an alternative of a multi-pass configuration was applied as illustrated in Fig. 3(a), which basically worked by making the control field go through the crystal for multiple times [69, 77, 78[. Figure 3(b) depicts the experimentally determined light storage efficiency η_{EIT} versus the signal pulse duration τ_p and the control power P_c ($P_c \propto \Omega_c^2$) for a single pass ($N_{pass} = 1$) and a multipass setup ($N_{pass} = 10$). By applying the iterative pulse shaping algorithm developed and first implemented by Novikova *et al.* [79, 80] for a multi-pass setup, a storage efficiency of 76.3% was achieved $N_{pass} = 14$ [77]. The maximum achievable efficiency is limited by the finite loss from crystal surfaces. Further, errors caused by the environmental perturbation are accumulated in a long beam path, deteriorating the spin wave shape, resulting in a storage efficiency that is lower than the theoretically expected value [68]. As we know, there are yet no reports of EIT storage on single photon level in a doped solid. Rencently, Hain *et al.* [70] used double pass setup

to successfully store a few photons. They achieved a maximum storage efficiency of 1.7% after a storage time of 10s with an average number of photons $\overline{n} = 53$ [70] [see Fig. 3(c)]. In a coherent optical storage experiment, the strong control beam and the stored signal are almost collinear. In this situation, it is difficult to filter the scattered noise and coupled noise photons in the control beam. Meanwhile, the phase mismatching caused by the large angle separation leads to strong four-wave mixing (FWM), significantly degrading the purity of a single photon state [76, 81–83]. With the above limitations, the weakest light signal was supposed to be more than 10 photons to ensure a reasonable SNR.

The time multi-mode capability of the EIT protocol, given by the width of its transparent window, is limited to a few MHz. However, its angular multiplexing in the storage and retrieval light pulse has allowed demonstrations of saving an image, which was realized first in rubidium vapor [84, 85] and then also in RE crystals [86, 87]. A spatially real image was stored in an RE crystal, instead of Fourier image, as was demonstrated in a gas medium. This reduces the loss of information caused by the fact that the control beam does not cover the higher frequency component of the Fourier spectrum [84], leading to superior quality of the retrieved image. In 2013, Heinze *et al.* [71] extended EIT storage times to one minute by applying dynamic decoupling (DD) pulse sequence to fight decoherence in the relevant spin transition, as shown in Fig. 3(d).

In summary, the current progress in RE crystals based EIT protocol mainly achieved on the storage of classical signals. The main challenge in storing quantum information comes from the media's low optical depth. Cavity enhancement has been proved to be a feasible solution while in practical experiment, designing a suitable cavity involves various complex tasks and increasing the complexity of the experimental process [88]. Errors from an imperfect cavity and a complicated controlling system can be accumulated and cause further decoherence and a worse SNR. In addition, EIT storage scheme is based on homogenous broadening of a media, limiting its maximum achievable storage capacity. In contrast, storage protocols based on the idea of photon echo allows using a media's inhomogeneous broadening for multi-mode storage under a given optical depth.

4 Photon echo memories

In an RE crystal, a dopant ion inevitably experience static variations in the strain, electric or magnetic field from site to site, causing an inhomogeneous distribution of the dopant's transition frequencies, which generally ranges from 1–30 GHz, depending on the doping concentration and fabrication processes. A memory protocol using this inhomogeneous broadening allows prospective capacity of multiple mode storage and a typical example is the photon echo memories. In contrast to the EIT protocol, photon echo memories generally work by applying a time-reversed absorption process, instead of making the sample transparent [89].

Coherent manipulation and storage of classical light states using photon echo (PE) techniques dates back to the 1980s [90, 91]. An initially polarized ensemble of atoms, which are inhomogeneously broadened, is excited to a superposition of two levels by applying an optical $\pi/2$ pulse, creating a collective dipole moment. The static detuning in the transition frequency among the different subgroups of atoms leads to a decay in the collective dipole moment. An optical π pulse after a delay τ reverse the atom population between the ground state and the excited state, resulting in a refocusing of the collective dipole moment of the system at a delay of 2τ, irradiating as an echo signal. The phase accumulation due to the static detuning during the dephasing and rephasing intervals cancels, thus the echo amplitude is governed by the dynamic contribution. As the optical version of the Hahn spin echo, the photon echo technique have been widely used in the spectroscopic studies for optical materials and in classical optical memory applications [92].

However, a standard PE scheme is not suitable for storing quantum information. In a quantum regime, the incoming signal is an arbitrarily weak field, whose quantum feature can be easily buried in the noise from the amplified spontaneous emission induced by the applied π pulse [93–96]. Hence, various proposals were applied to tackle with this issue, some of which have been experimentally proved to be very effective. In this section, we will briefly introduce two typical proposals and the relevant research progress, including controlled reversible inhomogeneous broadening (CRIB) [97] and atomic frequency comb (AFC) [98].

4.1 Controlled reversible inhomogeneous broadening (CRIB) and gradient-echo memory (GEM)

The fundamental principle of a CRIB scheme is to manipulate the inhomogeneous broadening through a controllable magnetic or electric field, such that the phase of the collective dipole moments is refocused to its initial value at 2τ. Under a controlled excitation, all atoms will then irradiate light coherently. In contrast to a PE scheme, no rephasing π pulse is used to inverse the population.

Typically, CRIB can be realized by using an electric field to induce an extra broadening in an initially homogeneously broadened ensemble of atoms [100, 101]. After a waiting period that is shorter than the system's coherence time, the electric field is inverted, accordingly the coherence evolution of the system is inverted. Depending on whether the applied field is perpendicular to or along

the direction of light propagation, it is called a "transverse" CRIB or a "longitudinal" CRIB. For the former, theoretical model shows that the maximum achievable storage efficiency is limited to 54% due to the re-absorption by RE ions [102]. The "longitudinal" CRIB often refers to a gradient echo memory (GEM) as shown in Fig. 4. Applying an electric field gradient along the direction of the light propagation prevents the output echo from being reabsorbed, allowing an ideal echo emission and a storage efficiency upper limit of 100% [99, 103].

In 2006, an experimental result of CRIB storage in a solid-state system was reported for the first time, yet with a low storage efficiency. In this work, the applied material system, an Eu^{3+}:YSO crystal, experienced a linear Stark shift and macroscopic electric field gradient [97, 104]. The efficiency was extended to 15% in a later experiment [103]. In 2010, CRIB storage and on-demand retrieval of a weak beam at telecommunication wavelength was demonstrated in an Er^{3+}:YSO crystal, with average photon number of one. In this experiment, a second laser beam was used to transfer the states of atoms down to a short-lived ground state from the excited state, which improved the degree of spin polarization and reduced the fluorescence noise arising from the state preparation process [107]. However, due to the imperfect optical pumping [Fig. 5(a)], the large background absorption ($\sim 80\%$) and reabsorption process limited the storage efficiency to 0.25%. In 2010, a GEM-based memory demonstrated a storage efficiency of 69% for a weak coherent light signal [108] [the solid line in Fig. 5(b)], which was for the first time beyond the no-cloning limit [109]. The experiment is performed in a 0.005% Pr^{3+}:YSO. Given the long ground state lifetime, a 140 dB absorptive top-hat profile was created with a more efficient optical pumping. According to the theoretical model, and considering a perfect optical pumping process, Hedges *et al.* [106] predicted that it is possible to achieve a peak efficiency of about 93% if the crystal length was 10 cm instead of 14 mm.

We have briefly introduced the two-level CRIB protocol and especially its "longitudinal" variant, namely the GEM protocol. Although the theoretical model shown an efficiency of 100% for a GEM-based quantum memory is possible, it can be challenging to get close to this limit for RE crystals, given by the low absorption depth [110–115]. We can optimize the optical pumping process to reduce the background absorption and increase the number of effective atoms. An alternative way is to use

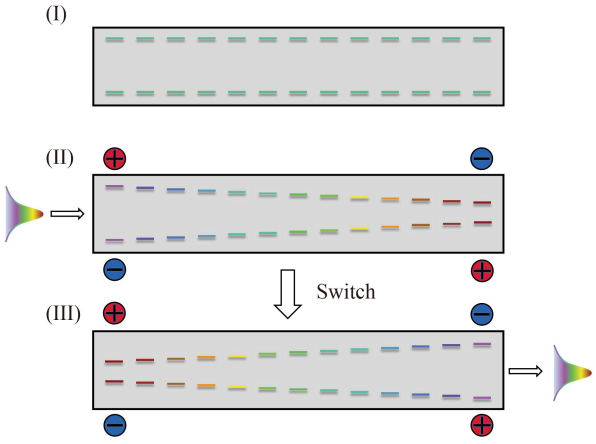

Fig. 4 Schematic of the GEM protocol. (I) An ensemble of identical two level atoms is prepared; (II) A linear Stark shift is applied, thereby allowing the medium to absorb the different part of input pulse; (III) After switching the polarity of the electric field, the input pulse comes out as an echo. This figure is reproduced from Ref. [99].

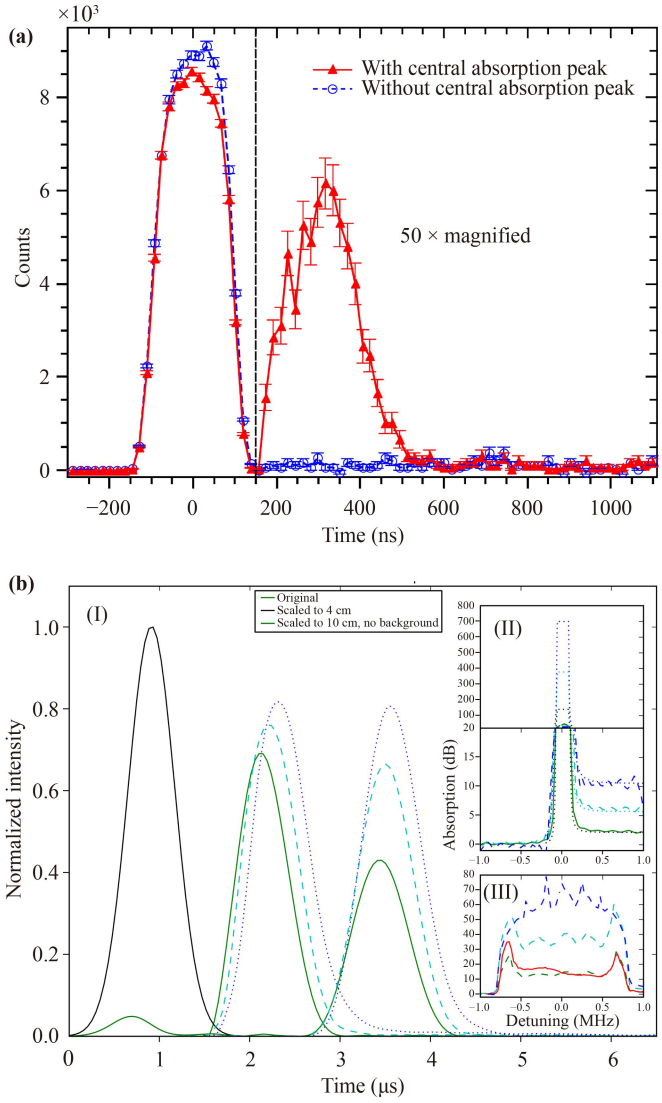

Fig. 5 **(a)** Experimental demonstration of CRIB storage [105]. **(b)** Experimental result (solid line) and predicted echoes by simply scaling the media to 4 cm (dash line) and 10 cm (dotted line); (I) Input and retrieved echo; (II) Absorption spectrum of the prepared feature; (III) Absorption spectrum when the field was not switched to retrieve the echo [106].

stoichiometric RE crystals to increase the density [116–118]. Although the achieved storage efficiency is as high as 69%, the storage bandwidth of Pr^{3+} is limited to ~ 5 MHz due to the low nuclear quadrupole interaction. Among the many rare earth crystals, there are some systems with a larger nuclear quadrupole moments, such as Eu^{3+}:YSO. In Eu^{3+}:YSO, the bandwidth is about ~5.7 MHz for $^{151}Eu^{3+}$ and ~15 MHz for $^{153}Eu^{3+}$ respectively [119].

In addition to its application in quantum storage, GEM has also been proposed to realize quantum state transfer by performing time reversal operation [120]. The advantage is that the collective excitation of the ensemble is beneficial to the fidelity of the quantum state that is transferred and there is no need for strong coupling between a high-Q cavity and the atoms that make up the nodes of a given quantum network [121]. We will not go into too much detail here.

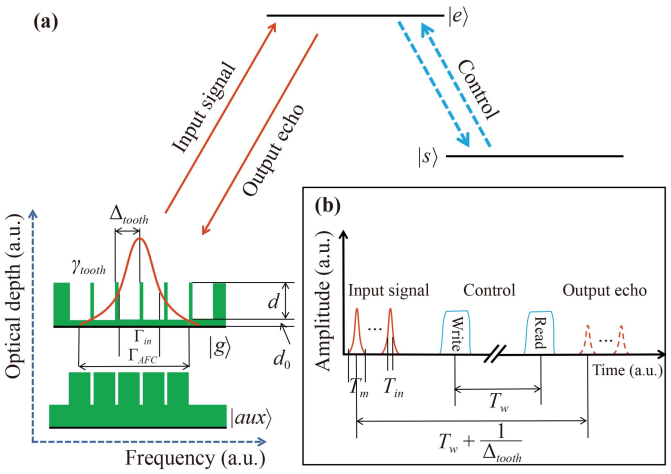

Fig. 6 Schematic of the AFC protocol. Reproduced from Ref. [122].

4.2 Atomic frequency comb (AFC)

In practical large-scale quantum network applications, the multi-mode capacity of a quantum memory is imperative because it can dramatically accelerate communication. RE solid-state ensembles allows the potential for multiplex storage in frequency, time, space and polarization mode. However, it can be experimentally challenging using EIT or CRIB scheme, limited by the optical depth. [123]. In contrast, the atomic frequency comb (AFC) protocol can achieve multi-mode storage with a relatively low optical depth [122].

The AFC protocol was first proposed by de Riedmatten *et al.* [98] in 2008 and it grounded in the large ratio between the inhomogeneous and homogeneous linewidth of an RE crystal, which is 10^5–10^8 typically. In the broad inhomogeneous profile, a series of absorption peaks, namely a frequency comb, are produced through the hole-burning technique. As shown in Fig. 6(a), it works by burning a series of narrow holes in the atomic medium. The ions, pumped to the metastable $|aux\rangle$ level are then no longer couple to the incoming field. This comb-like absorption profile is characterized by two parameters: peak separation Δ_{tooth} and peak width γ_{tooth}. With an absorption of an incoming photon (at $t = 0$), whose waveform spanned over the frequency comb, the state of the signal is converted into a collective excitation in the form [127]:

$$|\Psi(t)\rangle = \frac{1}{\sqrt{N}} \sum_{j=1}^{N} c_j \mathrm{e}^{2\pi \mathrm{i} \Delta_j t} \mathrm{e}^{-\mathrm{i} k_j z_j} |g_1 .... e_j ... g_N\rangle ., \qquad (8)$$

where $\Delta_j \approx m\Delta_{tooth} (m \in \mathbb{Z}$, the peak order) and z_j are the frequency and position of the jth ion in the ensemble. Given the periodic property of the medium, after the initial dephasing, the phase of all the excited ions will automatically refocus at $t = \frac{n}{\Delta_{tooth}} (n \in \mathbb{Z})$ and coherently irradiate light signal. Here high-order echoes ($n > 1$) are in theory possible, but they tend to have a much lower SNR [127], so only the first-order echo was considered. It is worth noting that for a two-level AFC protocol as discussed above, the storage time is predefined so it is not possible for on-demand recall. On demand recall can be realized by transferring the excitation to another metastable state $|s\rangle$ with a control field, namely the spin-wave storage.

There have been impressive AFC demonstrations since it was proposed, including coherent preservation of polarization qubit states [128–133], herald photons memories [134–142], etc. In this section, we will focus on discussing the recent research progress of the AFC-based memory, from the perspective of each storage performance.

4.2.1 Multi-mode storage

If the input signal pulse duration T_m is much shorter than the fixed storage time $\frac{1}{\Delta_{tooth}}$, multi-mode temporal storage $N_t = \frac{1}{\Delta_{tooth} T_m}$ is possible [see Fig. 6(b)]. For a short input pulse of a duration time Tm, AFC bandwidth of $\Gamma_{AFC} > \frac{2.5}{T_m}$ is required [119]. Thus, the temporal multi-mode capacity in the fixed storage time $\frac{1}{\Delta_{tooth}}$ is written as

$$N_t = \frac{1}{\Delta_{tooth} T_m} = \frac{\Gamma_{AFC}}{2.5\Delta_{tooth}} \approx \frac{N_{tooth}}{2.5}, \qquad (9)$$

where $N_{tooth} = \frac{\Gamma_{AFC}}{\Delta_{tooth}}$ is the number of the peaks in the AFC profile.

In 2008, de Riedmatten *et al.* [98] realized four temporal modes storage at single-photon level. After this pineering work, 64 weak coherent pulses in the time domain were coherently mapping in a Nd^{3+}:YSO [124] system [see Fig. 7(a)] Tang *et al.* [143] demonstrated a storage of 100

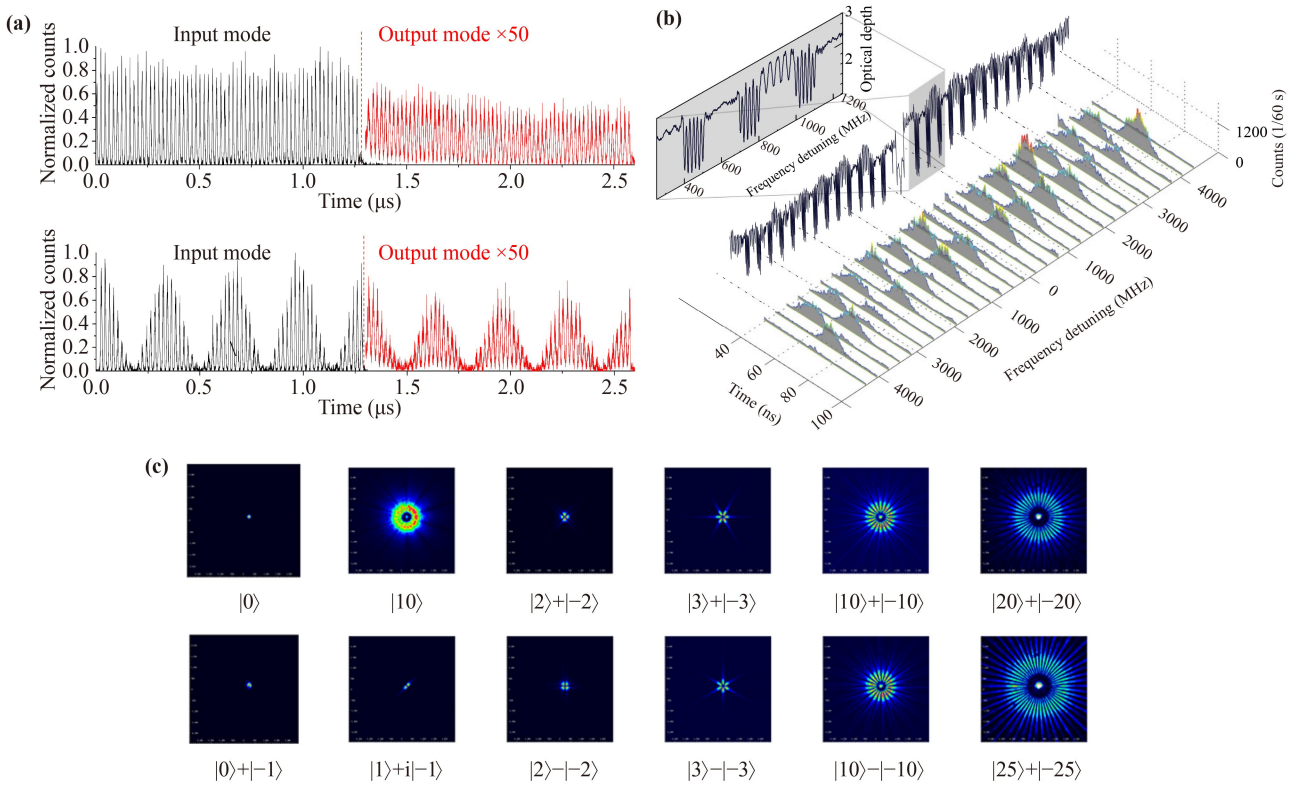

Fig. 7 Experimental demonstration of different multi-mode storage with AFC protocol. **(a)** Two examples of storage of 64 optical temporal modes with different input sequences [124]. **(b)** Multiple frequency mode storage and selective recall [125]. **(c)** Examples of measured intensity profiles of orbital-angular-momentum (OAM) as an outstanding spatial multi-mode operations [126].

temporal modes in a hybrid solid state system, where a $Nd^{3+}:YVO_4$ crystal is used to store the polarization encoded single photons emitted from quantum dots. Further, there were also demonstrations to encode each pair of temporal modes as a time-bin qubit, which was widely used in fiber-based quantum communication due to their resilience against polarization decoherence in fibers [144–146].

In a system with a short coherence time, the decoherence term $\eta_{T_2} = e^{-\frac{4}{\Delta T_2}}$ need to be included when estimating the multi-mode capacity during the actual storage time $\frac{1}{\Delta_{tooth}}$, Eq. (9) is then rewritten as [119]

$$N_t \approx \frac{\ln(1/\eta_{T_2})}{10}\Gamma_{AFC}T_2. \tag{10}$$

In this equation, $\Gamma_{AFC}T_2$ represents the time-bandwidth product of a AFC memory. Kramer ions, such as Nd^{3+} or Er^{3+}, usually possesses a larger bandwidth Γ_{AFC} but a shorter coherence time as a result of the non-zero electron spin, which limits the mode capacity. In contrast, non Kramer ions can have longer coherence time. The Eu^{3+}:YSO crystal is a very typical non-Kramer RE system, where Jobez *et al.* [147] achieved storage of 100 temporal modes and at the same time a long storage time ($\frac{1}{\Delta_{tooth}}$). However, non-Kramer ions usually have a smaller hyperfine splittings which limits the AFC bandwidths Γ_{AFC}. About Kramer RE systems, there is a very unique Yb^{3+}:YSO system, with hyperfine splittings of hundreds MHz to GHz [148], demonstrated both long optical and spin coherence time at the low-field clock transitions [149].

In a storage experiment, the number of combs required to be prepared increases linearly with mode number. Applying sequential hole burning technique to prepare a large number of combs takes a long time and can raise the temperature of the system, resulting in instantaneous spectral diffusion and extra decoherence [150]. A solution to this issue is to apply a parallel comb preparation technique [147], which works by using a phase and amplitude modulated pulse, appearing as a periodic squarish frequency comb profile in the Fourier domain. The parallel comb preparation technique not only mitigate the heating problem, but also improves the resolution of the combs by modifying the Fourier limitation. Using such a method in Yb^{3+}:YSO, it realized over 1250 storage modes [151]. Such a high mode capacity can greatly enhances the communication rate in a large-scale quantum networks.

The large inhomogenous broadening of RE doped crystals provides intrinsic advantage for spectral multi-modality of up to $N_f = \frac{\Gamma_{inh}}{\Gamma_{AFC}}$, which work by tailoring AFC profile at different site across the static broadening

to absorb photons of different energies. Sinclair *et al.* [125] first demonstrated spectral AFC multiplexing based in $Ti^{3+}:Tm^{3+}:LiNbO_3$ with each mode encode by a time bin qubit [see Fig. 7(b)]. Then heralded single photons were shown to be manipulated for time-frequency multiplexing storage [152–154]. Furthermore, the Orbital Angular Momentum (OAM) of photons have been shown to possess outstanding degree of freedom in carrying high-dimensional entanglement and spatial multi-mode operations [126]. The storage result is sketched out in Fig. 7(c).

4.2.2 Efficient storage

The storage and retrieval efficiency of an AFC-based quantum memory can be written as [122]

$$\eta_{AFC} = \tilde{d}^2 e^{-\tilde{d}} e^{-d_0} e^{\frac{-7}{F^2}}, \tag{11}$$

where $F = \frac{\Delta_{tooth}}{\gamma_{tooth}}$ is defined as the finesse of the comb and $\tilde{d} \approx \frac{d}{F}$ is the effective absorption considering that the number of atoms interacting with the signal is reduced because of the comb profile. The four terms at the right side of the equation represent respectively the effect of atom-light coupling, resorptive effect, background absorption and the dephasing due to the broadening of a peak in the comb. The first term is a square term because both absorption and the reemission of the field is taken into account.

For a forward reemission, the reabsorption process limits the efficiency up to 54%. The backward retrieval does not have this issue but it requires a pair of accurate π pulse, which can be experimentally very difficult [158]. A promising strategy to improve efficiency is to apply an impedance matched cavity to enhance light matter interaction. Technically, impedance matching of a Fabry–Pérot (FP) cavity, for instance, requires the reflection of both mirror to satisfy $\sqrt{R_1} = R_2 e^{-\tilde{d}}$ [159, 160]. With an optical cavity, Sabooni *et al.* [155] and Jobez *et al.* [161] demonstrated AFC storage for classical light with an efficiency of 53% in Eu^{3+}:YSO and 56% in Pr^{3+}:YSO respectively. For the latter, 16% of the energy was not absorbed due to the impedance mismatching as shown in Fig. 8(a).

Research of a quantum memory often use input photons produced through spontaneous parametric down conversion (SPDC) process, which can have a broad bandwidth, causing difficulty to impedance matching of a cavity. A recent research in $Tm^{3+}:Y_3Al_5O_{12}$ has demonstrated enhanced absorption over a wide spectral range by using a low finesse cavity and achieved 90% absorption of the input photons, leading to a storage efficiency of 27.5% as well as 1.6 GHz bandwidth [162]. It was argued that higher efficiency is possible by optimizing impedance matching and filtering the broad SPDC photons. Again, applying cavity enhanced AFC protocol, Duranti *et al.* [163] reported successful storage of weak

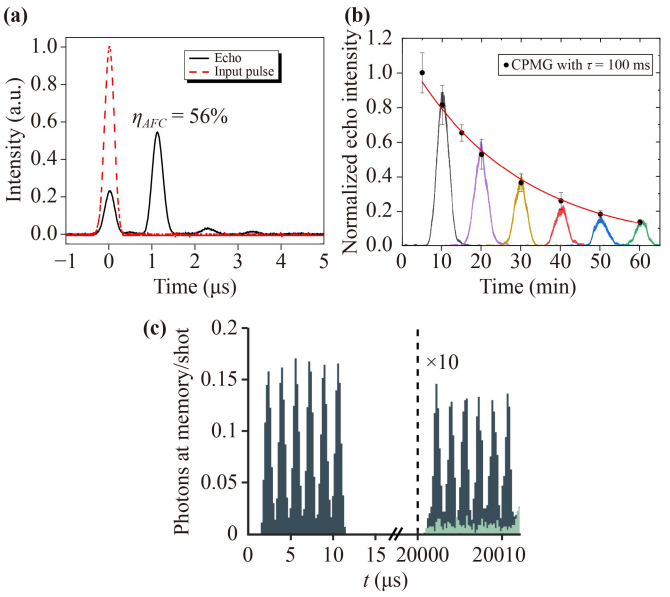

Fig. 8 Experimental demonstration of AFC. **(a)** Relationship between output echo and corrected input pulse (red dash line) at 1.1 μs gives a storage efficiency $\eta_{AFC} = 56\%$ using cavity enhancement AFC protocol [155]. **(b)** The decay of the spin-wave AFC echo intensity using CPMG sequence with $\tau = 100$ ms versus the storage time. The signal was still visible after an hour [156]. **(c)** The spin-wave AFC stores three time-bin qubits after 20 ms for $\eta = 7.39\%$ [157].

coherent states and weak coherent time-bin qubits with efficiency of up to 62% and 51% respectively. It was conducted in a Pr^{3+}:YSO crystal, and the absorption depth was $\tilde{d} = 0.4$, which limited by the intra cavity losses and cavity bandwidth.

As we mentioned, on demand retrieval in an RE system can be realized through spin-wave AFC storage, which works by applying a π pulse to transfer the excitation to an auxiliary level, usually meaning another long-lived spin state. Then the total efficiency can be expressed as $\eta = \eta_{AFC}\eta_t^2$ [164], where η_t is the population transfer efficiency, and the decoherence of the spin state is ignored because it is slow in most cases. In order to raise population transfer efficiency, people have designed some special pulse sequences, two typical examples are the complex hyperbolic secant(CHS) pulse [165, 166] and the hyperbolic-square-hyperbolic (HSH) pulse [167]. In theory, a transfer efficiency of 100% is possible [165] and the actual efficiency realized is 90% per HSH pulse [168].

4.2.3 Long-term storage

For a memory to be useful in a quantum network, its storage time must be comparable to the total light transmission times across the communication network. The storage time of a memory is limited by the transition's coherence time. In RE systems, the application of spin-wave AFC protocol [164], provides not only on-

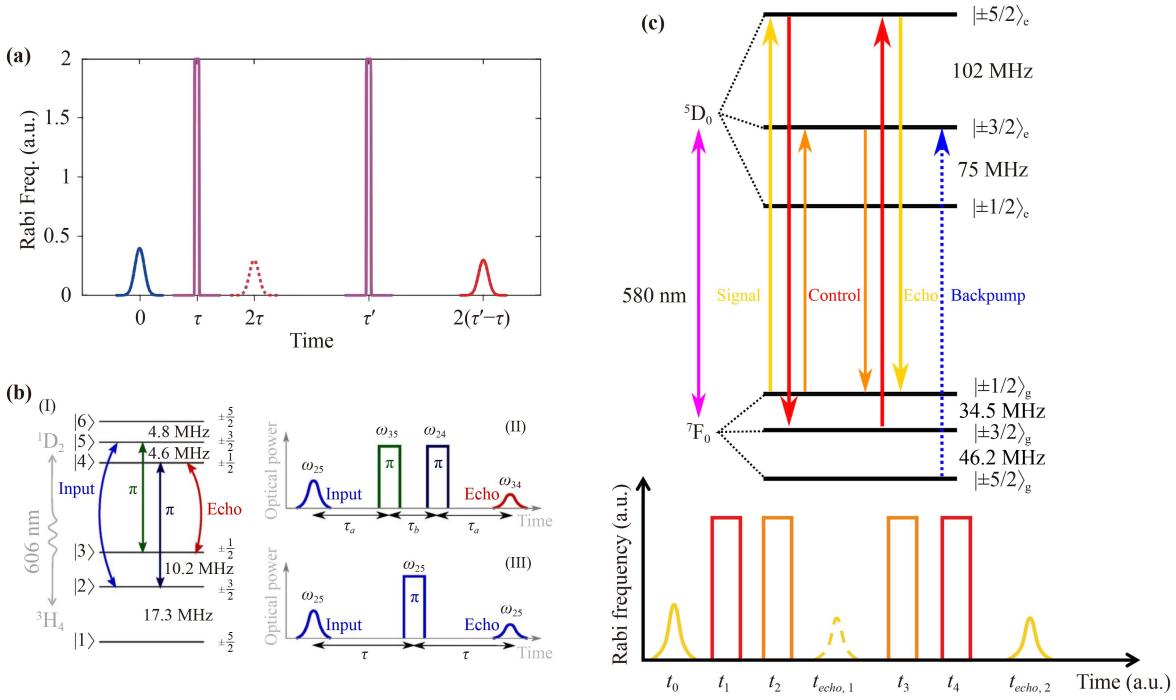

Fig. 9 **(a)** Schematic diagram of ROSE protocol sequence [56]. The first echo at $t = 2\tau$ is suppressed by the phase matching conditions: $k_{echo,1} = 2k_1 - k_0$. The secondary echo is emitted at time $t = 2(\tau' - \tau)$, satisfying the phase matching condition $k_{echo,2} = k_0 + 2(k_1 - k_2)$, where k_0, k_1, k_2 are the wavevectors of input signal, first π pulse and second π pulse respectively. **(b)** Energy level diagram and experimental sequence [169]. (I) Energy-level structure of experimental Pr^{3+}:YSO and experimental transitions. (II) Pulse sequence for the 4LE, with transition frequencies marked on the left. (III) Comparison to standard 2PE pulse sequence. **(c)** Energy level structure of $^{151}Eu^{3+}$:YSO crystal and experimental sequence of NLPE [170]. Same as shown in Fig. 9(a), the first echo at time $t = t_0 + t_1 - t_2$ is silenced by the phase matching condition: $k_{echo,1} = k_1 + k_2 - k_0$. The phase matching condition for NLPE echo at time $t = t_0 - t_1 - t_2 + t_3 + t_4$ is $k_{echo,2} = k_0 - k_1 - k_2 + k_3 + k_4$. Where, the k_i represents the wavevector of each input pulse at time t_i respectively.

demand storage but also longer storage time, which is given by the hyperfine coherence, and usually longer than the optical coherence time. Storage time of the spin-wave AFC protocol is then written $T_{total} = T_w + \frac{1}{\Delta_{tooth}}$, where T_w is the wait time.

In order to obtain a longer storage time, various strategies have been used to extend the hyperfine coherence times. It has been shown that long spin coherence times can be achieved in some Kramers RE ions with strong mixing of electron spin and nuclear spin. Spin coherence time of several millisecond at zero or weak applied magnetic field was observed in such systems [149, 171]. Applying a strong magnetic field of seven Tesla even resulted in a hyperfine coherence time of 1.3 s in Er^{3+}:YSO [172]. In a non-Kramer RE system, Eu^{3+}:YSO, a combined effect of a ZEFOZ transition and DD pulses extended the hyperfine coherence time from 10 ms to 6 hours [44, 173]. This same ZEFOZ transition was used for a spin-wave AFC storage, which realized storage of classical optical signal for one hour [156] [Fig. 8(b)]. Integration of spin-wave AFC storage and DD have resulted in storage of time-bin qubits for 20 ms [157] [see Fig. 8(c)].

4.3 Other protocols

Some other PE-based storage protocols have been proposed in RE doped systems. The main issue with a single PE sequence is that the applied π pulse resulted in a population-inverted medium, irradiating noise to the echo signal. The fundamental principle of the revival of silenced echo (ROSE) protocol, as illustrated in Fig. 9(a), works by applying a second π pulse to transfer the population back to the initial state, rephasing the induced dipole for the second time and irradiating the signal coherently without amplification noise [174–176]. It is worth noting that the rephasing π pulses are in practice replaced by complex hyperbolic secant (CHS) pulses. In addition, the first echo become a "silenced echo" because special phase matching conditions are designed such that when the first rephasing occurs, no field emission is produced, but the coherent free evolution continues. Using a ROSE protocol, optical storage efficiency of 40% in an Er^{3+}:YSO was demonstrated [177].

The major challenge in an ROSE protocol is that imperfect π pulses lead to a large residual ensemble coherence, the free induction decay (FID), which possess the same spatial and frequency mode as the π pulses,

destructing SNR for single photon-level storage. As illustrated in Fig. 9(b), the "four-level echo" (4LE) protocol employs a double-Λ energy level setup to transfer the input coherence to a different transition such that the FID noise can be frequency filtered from the echo signal [169]. The 4LE pulse sequence also allows off-axis phase matching, implying possibility for spatial filtering for the signal. It demonstrated a PE level of storage efficiency, but the coherence is reduced by the inhomogeneity caused by using four transitions.

The noiseless photon-echo (NLPE) scheme, proposed by Ma *et al.* [170], can be considered as an integration of ROSE and 4LE. It employs symmetrical 4LE configuration to conduct double rephasing and it satisfies the phase matching condition to silence the echo generated by 4LE. This is illustrated more in Fig. 9(c). The NLPE protocol is possible to obtain higher storage efficiency and SNR than the AFC protocol because it does not need the spectral tailoring process. However, due to the limited storage time in the excited state, optical depth and the bandwidth limit caused by the instantaneous spectral diffusion, NLPE still has a lower multi-mode capacity compared to AFC [178, 179]. Further, the symmetrical 4LE configuration involves a considerable number of control pulses, which can introduce more complexity for cavity enhancement.

The last protocol we are to discuss is the Stark-modulated atomic frequency comb (SMAFC) protocol, proposed by Horvath *et al.* [180–183], which has demonstrated multi-mode storage capability and on-demand retrieval on a two level system. With this protocol, no irreversible dephasing is produced by the two electric field control pulses. Hence, it can be integrated to the cavity enhanced AFC protocol and will allow on-demand storage without additional optical control pulses.

We have presented a brief introduction of the quantum memory protocols, derived from the two pulse photon echo technique. The GEM is remarkable for its efficiency and AFC for its high multimode capacity, both verifies the appealing prospect for a practical quantum memory, if cavity enhancement is optimized. Among all the different RE ions, non-Kramer ions tend to provide longer coherence time while Kramer ions can provide greater bandwidth and mode capacity.

5 Conclusion and outlook

Construction of a quantum network is an important and challenging goal in the field of quantum information, which requires integration of a series of functional quantum devices, including quantum memories, photon pair sources, frequency adapters and quantum sensors, to name a few. In terms of developing quantum memories, a number of different material systems have been investigated, but no system has yet demonstrated all the required performances for a memory to be practical.

In this review, we focused on a particular system, the RE crystals and have briefly summarized its experimental progress on the development of quantum storage devices. Remarkable storage performances has been demonstrated, such as an efficiency of 69%, storage mode number of 1250 and storage time of 20 ms. Recently, RE systems were also demonstrated to be used for storing hyper-entangled and high dimensional quantum states (qudits), which can enable more efficient Bell state measurements and simplify purification procedure [126, 184–187]. However, for majority of the mentioned storage protocols, there is a main limitation for better performances, that is the system's low optical depth. To preserve good coherence property, storage experiments tend to use a dilutedly doped sample and apply an impedance matched cavity to enhance its optical depth. The reality is, optimizing impedance matching for a cavity is technically not easy, especially in a situation when the input photon source has a large bandwidth, for instance, the SPDC source.

In practical application, interfacing a quantum memory with an entangled photon source is a very common challenge. For RE-based quantum memories, some elegant solutions, based on rephased amplified spontaneous emission (RASE) [188–193] and AFC-DLCZ [194–198], have been successfully demonstrated. Through such strategies, entangled photon pair source can be generated from an RE system that is used as a memory. In most cases, the source and the memory are from different systems and a hybrid configuration is alternative. An RE-based memory has demonstrated successful interfacing to an efficient quantum dot system [143], the latter of which has shown the potential to realize narrower and faster emission through cavity enhancement [199–201].

As solid, RE crystals have also demonstrated its advantage of being easy to integrate with other systems. At present, some groups are carrying out research work in this field and have made many breakthroughs as detailed in the following references [176, 202–209].

Acknowledgements This work was supported by the National Natural Science Foundation of China (Grant Nos. 11904159 and 12004168), Guangdong Basic and Applied Basic Research Foundation (Grant No. 2021A1515110191), Guangdong Innovative and Entrepreneurial Research Team Program (Grant No. 2019ZT08X324), the Guangdong Provincial Key Laboratory (Grant No. 2019B121203002), and the Key-Area Research and Development Program of Guangdong Province (Grant No. 2018B030326001).

References

1. M. A. N. L. Chuang, Quantum Computation and Quantum Information, Cambridge University Press, Cambridge, 2010

2. M. Vogel, Quantum computation and quantum information, by M. A. Nielsen and I. L. Chuang, *Contemp. Phys.* 52(6), 604 (2011)
3. P. Zoller, T. Beth, D. Binosi, R. Blatt, H. Briegel, D. Bruss, T. Calarco, J. I. Cirac, D. Deutsch, J. Eisert, A. Ekert, C. Fabre, N. Gisin, P. Grangiere, M. Grassl, S. Haroche, A. Imamoglu, A. Karlson, J. Kempe, L. Kouwenhoven, S. Kröll, G. Leuchs, M. Lewenstein, D. Loss, N. Lütkenhaus, S. Massar, J. E. Mooij, M. B. Plenio, E. Polzik, S. Popescu, G. Rempe, A. Sergienko, D. Suter, J. Twamley, G. Wendin, R. Werner, A. Winter, J. Wrachtrup, and A. Zeilinger, Quantum information processing and communication, *Europ. Phys. J. D* 36, 203 (2005)
4. N. Gisin, G. Ribordy, W. Tittel, and H. Zbinden, Quantum cryptography, *Rev. Mod. Phys.* 74(1), 145 (2002)
5. C. L. Degen, F. Reinhard, and P. Cappellaro, Quantum sensing, *Rev. Mod. Phys.* 89(3), 035002 (2017)
6. I. M. Georgescu, S. Ashhab, and F. Nori, Quantum simulation, *Rev. Mod. Phys.* 86(1), 153 (2014)
7. S. Wehner, D. Elkouss, and R. Hanson, Quantum internet: A vision for the road ahead, *Science* 362(6412), eaam9288 (2018)
8. H. J. Kimble, The quantum internet, *Nature* 453(7198), 1023 (2008)
9. S. H. Wei, B. Jing, X. Y. Zhang, J. Y. Liao, C. Z. Yuan, B. Y. Fan, C. Lyu, D. L. Zhou, Y. Wang, G. W. Deng, H. Z. Song, D. Oblak, G. C. Guo, and Q. Zhou, Towards real-world quantum networks: A review, *Laser Photonics Rev.* 16(3), 2100219 (2022)
10. C. H. Bennett and G. Brassard, Quantum cryptography: Public key distribution and coin tossing, *Theoretical Computer Science* 560, 7–11 (2014), Theoretical Aspects of Quantum Cryptography-celebrating 30 years of BB84
11. F. Xu, X. Ma, Q. Zhang, H. K. Lo, and J. W. Pan, Secure quantum key distribution with realistic devices, *Rev. Mod. Phys.* 92(2), 025002 (2020)
12. A. Boaron, G. Boso, D. Rusca, C. Vulliez, C. Autebert, M. Caloz, M. Perrenoud, G. Gras, F. Bussières, M. J. Li, D. Nolan, A. Martin, and H. Zbinden, Secure quantum key distribution over 421 km of optical fiber, *Phys. Rev. Lett.* 121(19), 190502 (2018)
13. J. P. Chen, C. Zhang, Y. Liu, C. Jiang, W. Zhang, X. L. Hu, J. Y. Guan, Z. W. Yu, H. Xu, J. Lin, M. J. Li, H. Chen, H. Li, L. You, Z. Wang, X. B. Wang, Q. Zhang, and J. W. Pan, Sending-or-not-sending with independent lasers: Secure twin field quantum key distribution over 509 km, *Phys. Rev. Lett.* 124(7), 070501 (2020)
14. W. K. Wootters and W. H. Zurek, A single quantum cannot be cloned, *Nature* 299(5886), 802 (1982)
15. H. J. Briegel, W. Dür, J. I. Cirac, and P. Zoller, Quantum repeaters: The role of imperfect local operations in quantum communication, *Phys. Rev. Lett.* 81(26), 5932 (1998)
16. N. Sangouard, C. Simon, H. de Riedmatten, and N. Gisin, Quantum repeaters based on atomic ensembles and linear optics, *Rev. Mod. Phys.* 83(1), 33 (2011)
17. S. Muralidharan, L. Li, J. Kim, N. Lütkenhaus, M. D. Lukin, and L. Jiang, Optimal architectures for long distance quantum communication, *Sci. Rep.* 6(1), 20463 (2016)
18. Z. S. Yuan, X. H. Bao, C. Y. Lu, J. Zhang, C. Z. Peng, and J. W. Pan, Entangled photons and quantum communication, *Phys. Rep.* 497(1), 1 (2010)
19. K. Hammerer, A. S. Sørensen, and E. S. Polzik, Quantum interface between light and atomic ensembles, *Rev. Mod. Phys.* 82(2), 1041 (2010)
20. E. Gouzien and N. Sangouard, Factoring 2048-bit RSA integers in 177 days with 13436 qubits and a multimode memory, *Phys. Rev. Lett.* 127(14), 140503 (2021)
21. Z. L. Xiang, S. Ashhab, J. Q. You, and F. Nori, Hybrid quantum circuits: Superconducting circuits interacting with other quantum systems, *Rev. Mod. Phys.* 85(2), 623 (2013)
22. P. Kok, W. J. Munro, K. Nemoto, T. C. Ralph, J. P. Dowling, and G. J. Milburn, Linear optical quantum computing with photonic qubits, *Rev. Mod. Phys.* 79(1), 135 (2007)
23. L. M. Duan, M. D. Lukin, J. I. Cirac, and P. Zoller, Long distance quantum communication with atomic ensembles and linear optics, *Nature* 414(6862), 413 (2001)
24. J. Hofmann, M. Krug, N. Ortegel, L. Gérard, M. Weber, W. Rosenfeld, and H. Weinfurter, Heralded entanglement between widely separated atoms, *Science* 337(6090), 72 (2012)
25. B. Hensen, H. Bernien, A. E. Dréau, A. Reiserer, N. Kalb, M. S. Blok, J. Ruitenberg, R. F. L. Vermeulen, R. N. Schouten, C. Abellán, W. Amaya, V. Pruneri, M. W. Mitchell, M. Markham, D. J. Twitchen, D. Elkouss, S. Wehner, T. H. Taminiau, and R. Hanson, Loophole-free bell inequality violation using electron spins separated by 1.3 kilometres, *Nature* 526(7575), 682 (2015)
26. A. Delteil, Z. Sun, W. Gao, E. Togan, S. Faelt, and A. Imamoğlu, Generation of heralded entanglement between distant hole spins, *Nat. Phys.* 12(3), 218 (2016)
27. R. Riedinger, S. Hong, R. A. Norte, J. A. Slater, J. Shang, A. G. Krause, V. Anant, M. Aspelmeyer, and S. Gröblacher, Non-classical correlations between single photons and phonons from a mechanical oscillator, *Nature* 530(7590), 313 (2016)
28. C. Li, S. Zhang, Y. K. Wu, N. Jiang, Y. F. Pu, and L. M. Duan, Multicell atomic quantum memory as a hardware-efficient quantum repeater node, *PRX Quantum* 2(4), 040307 (2021)
29. Y. Yu, F. Ma, X. Y. Luo, B. Jing, P. F. Sun, R. Z. Fang, C. W. Yang, H. Liu, M. Y. Zheng, X. P. Xie, W. J. Zhang, L. X. You, Z. Wang, T. Y. Chen, Q. Zhang, X. H. Bao, and J. W. Pan, Entanglement of two quantum memories via fibres over dozens of kilometres, *Nature* 578(7794), 240 (2020)
30. M. Minder, M. Pittaluga, G. L. Roberts, M. Lucamarini, J. F. Dynes, Z. L. Yuan, and A. J. Shields, Experimental quantum key distribution beyond the repeaterless secret key capacity, *Nat. Photonics* 13(5), 334 (2019)
31. M. K. Bhaskar, R. Riedinger, B. Machielse, D. S. Levonian, C. T. Nguyen, E. N. Knall, H. Park, D.

Englund, M. Lončar, D. D. Sukachev, and M. D. Lukin, Experimental demonstration of memory-enhanced quantum communication, *Nature* 580(7801), 60 (2020)
32. Y. F. Pu, S. Zhang, Y. K. Wu, N. Jiang, W. Chang, C. Li, and L. M. Duan, Experimental demonstration of memory-enhanced scaling for entanglement connection of quantum repeater segments, *Nat. Photonics* 15(5), 374 (2021)
33. N. Jiang, Y. F. Pu, W. Chang, C. Li, S. Zhang, and L. M. Duan, Experimental realization of 105-qubit random access quantum memory, *npj Quantum Inform.* 5, 28 (2019)
34. G. Buser, R. Mottola, B. Cotting, J. Wolters, and P. Treutlein, Single-photon storage in a ground-state vapor cell quantum memory, *PRX Quantum* 3(2), 020349 (2022)
35. K. B. Dideriksen, R. Schmieg, M. Zugenmaier, and E. S. Polzik, Room-temperature single-photon source with near-millisecond built-in memory, *Nat. Commun.* 12(1), 3699 (2021)
36. O. Katz and O. Firstenberg, Light storage for one second in room-temperature alkali vapor, *Nat. Commun.* 9(1), 2074 (2018)
37. Z. Yan, L. Wu, X. Jia, Y. Liu, R. Deng, S. Li, H. Wang, C. Xie, and K. Peng, Establishing and storing of deterministic quantum entanglement among three distant atomic ensembles, *Nat. Commun.* 8(1), 718 (2017)
38. B. Jing, X. J. Wang, Y. Yu, P. F. Sun, Y. Jiang, S. J. Yang, W. H. Jiang, X. Y. Luo, J. Zhang, X. Jiang, X. H. Bao, and J. W. Pan, Entanglement of three quantum memories via interference of three single photons, *Nat. Photonics* 13(3), 210 (2019)
39. X. Y. Luo, Y. Yu, J. L. Liu, M. Y. Zheng, C. Y. Wang, B. Wang, J. Li, X. Jiang, X. P. Xie, Q. Zhang, X. H. Bao, and J. W. Pan, Postselected entanglement between two atomic ensembles separated by 12.5 km, *Phys. Rev. Lett.* 129(5), 050503 (2022)
40. Y. F. Pu, N. Jiang, W. Chang, H. X. Yang, C. Li, and L. M. Duan, Experimental realization of a multiplexed quantum memory with 225 individually accessible memory cells, *Nat. Commun.* 8(1), 15359 (2017)
41. L. Heller, P. Farrera, G. Heinze, and H. de Riedmatten, Cold atom temporally multiplexed quantum memory with cavity enhanced noise suppression, *Phys. Rev. Lett.* 124(21), 210504 (2020)
42. M. F. Askarani, A. Das, J. H. Davidson, G. C. Amaral, N. Sinclair, J. A. Slater, S. Marzban, C. W. Thiel, R. L. Cone, D. Oblak, and W. Tittel, Long-lived solid-state optical memory for high-rate quantum repeaters, *Phys. Rev. Lett.* 127(22), 220502 (2021)
43. Z. Q. Zhou, D. L. Chen, M. Jin, L. Zheng, Y. Z. Ma, T. Tu, A. Ferrier, P. Goldner, C. F. Li, and G. C. Guo, A transportable long-lived coherent memory for light pulses, *Sci. Bull. (Beijing)* (2022)
44. M. Zhong, M. P. Hedges, R. L. Ahlefeldt, J. G. Bartholomew, S. E. Beavan, S. M. Wittig, J. J. Longdell, and M. J. Sellars, Optically addressable nuclear spins in a solid with a six-hour coherence time, *Nature* 517(7533), 177 (2015)
45. G. Wolfowicz, F. J. Heremans, C. P. Anderson, S. Kanai, H. Seo, A. Gali, G. Galli, and D. D. Awschalom, Quantum guidelines for solid-state spin defects, *Nat. Rev. Mater.* 6(10), 906 (2021)
46. D. D. Awschalom, R. Hanson, J. Wrachtrup, and B. B. Zhou, Quantum technologies with optically interfaced solid-state spins, *Nat. Photonics* 12(9), 516 (2018)
47. C. Thiel, T. Böttger, and R. Cone, Rare-earth-doped materials for applications in quantum information storage and signal processing, *J. Lumin.* 131, 353 (2011)
48. R. M. Macfarlane, High-resolution laser spectroscopy of rareearth doped insulators: a personal perspective, *J. Lumin.* 100(1–4), 1 (2002)
49. R. Macfarlane and R. Shelby, Chapter 3 - Coherent Transient and Holeburning Spectroscopy of Rare Earth Ions in Solids, in: Spectroscopy of Solids Containing Rare Earth Ions, Modern Problems in Condensed Matter Sciences, Vol. 21, edited by A. Kaplyanskii and R. Macfarlane, Elsevier, 1987, pp 51–184
50. A. J. Freeman and R. E. Watson, Theoretical investigation of some magnetic and spectroscopic properties of rare-earth ions, *Phys. Rev.* 127(6), 2058 (1962)
51. N. J. Cerf, A. Ipe, and X. Rottenberg, Cloning of continuous quantum variables, *Phys. Rev. Lett.* 85(8), 1754 (2000)
52. S. Massar and S. Popescu, Optimal extraction of information from finite quantum ensembles, *Phys. Rev. Lett.* 74(8), 1259 (1995)
53. C. Simon, H. de Riedmatten, M. Afzelius, N. Sangouard, H. Zbinden, and N. Gisin, Quantum repeaters with photon pair sources and multimode memories, *Phys. Rev. Lett.* 98(19), 190503 (2007)
54. O. A. Collins, S. D. Jenkins, A. Kuzmich, and T. A. B. Kennedy, Multiplexed memory-insensitive quantum repeaters, *Phys. Rev. Lett.* 98(6), 060502 (2007)
55. K. F. Reim, J. Nunn, V. O. Lorenz, B. J. Sussman, K. C. Lee, N. K. Langford, D. Jaksch, and I. A. Walmsley, Towards highspeed optical quantum memories, *Nat. Photonics* 4(4), 218 (2010)
56. T. Chanelière, G. Hétet, and N. Sangouard, Quantum Optical Memory Protocols in Atomic Ensembles, Academic Press, 2018, Chapter 2, pp 77–150
57. K. F. Reim, P. Michelberger, K. C. Lee, J. Nunn, N. K. Langford, and I. A. Walmsley, Single-photon-level quantum memory at room temperature, *Phys. Rev. Lett.* 107(5), 053603 (2011)
58. J. Nunn, I. A. Walmsley, M. G. Raymer, K. Surmacz, F. C. Waldermann, Z. Wang, and D. Jaksch, Mapping broadband single-photon wave packets into an atomic memory, *Phys. Rev. A* 75(1), 011401 (2007)
59. S. E. Harris, J. E. Field, and A. Imamoğlu, Nonlinear optical processes using electromagnetically induced transparency, *Phys. Rev. Lett.* 64(10), 1107 (1990)
60. M. Fleischhauer, A. Imamoglu, and J. P. Marangos, Electromagnetically induced transparency: Optics in coherent media, *Rev. Mod. Phys.* 77(2), 633 (2005)
61. M. O. Scully and M. S. Zubairy, Quantum Optics, Cambridge University Press, 1997
62. E. Kuznetsova, O. Kocharovskaya, P. Hemmer, and M. O. Scully, Atomic interference phenomena in solids with a longlived spin coherence, *Phys. Rev. A* 66(6), 063802 (2002)

63. B. Ham, P. Hemmer, and M. Shahriar, Efficient electromagnetically induced transparency in a rare-earth doped crystal, *Opt. Commun.* 144(4-6), 227 (1997)
64. A. Turukhin, V. Sudarshanam, M. Shahriar, J. Musser, and P. Hemmer, First observation of ultraslow group velocity of light in a solid, in: Technical Digest, Summaries of papers presented at the Quantum Electronics and Laser Science Conference, Postconference Technical Digest, IEEE Cat. No. 01CH37172, 2001, pp 6–7
65. A. V. Turukhin, V. S. Sudarshanam, M. S. Shahriar, J. A. Musser, B. S. Ham, and P. R. Hemmer, Observation of ultraslow and stored light pulses in a solid, *Phys. Rev. Lett.* 88(2), 023602 (2001)
66. J. J. Longdell, E. Fraval, M. J. Sellars, and N. B. Manson, Stopped light with storage times greater than one second using electromagnetically induced transparency in a solid, *Phys. Rev. Lett.* 95(6), 063601 (2005)
67. S. L. McCall and E. L. Hahn, Self-induced transparency, *Phys. Rev.* 183(2), 457 (1969)
68. A. V. Gorshkov, A. André, M. D. Lukin, and A. S. Sørensen, Photon storage in Λ-type optically dense atomic media (ii): Freespace model, *Phys. Rev. A* 76(3), 033805 (2007)
69. D. Schraft, M. Hain, N. Lorenz, and T. Halfmann, Stopped light at high storage efficiency in a Pr^{3+}:Y_2SiO_5 crystal, *Phys. Rev. Lett.* 116(7), 073602 (2016)
70. M. Hain, M. Stabel, and T. Halfmann, Few-photon storage on a second timescale by electromagnetically induced transparency in a doped solid, *New J. Phys.* 24(2), 023012 (2022)
71. G. Heinze, C. Hubrich, and T. Halfmann, Stopped light and image storage by electromagnetically induced transparency up to the regime of one minute, *Phys. Rev. Lett.* 111(3), 033601 (2013)
72. M. Hainn, EIT light storage of weak coherent pulses in a doped solid, Ph.D. thesis, Technischen Universität Darmstadt, 2021
73. Y. F. Hsiao, H. S. Chen, P. J. Tsai, and Y. C. Chen, Cold atomic media with ultrahigh optical depths, *Phys. Rev. A* 90(5), 055401 (2014)
74. Y. W. Lin, H. C. Chou, P. P. Dwivedi, Y. C. Chen, and I. A. Yu, Using a pair of rectangular coils in the mot for the production of cold atom clouds with large optical density, *Opt. Express* 16(6), 3753 (2008)
75. Y. F. Hsiao, P. J. Tsai, H. S. Chen, S. X. Lin, C. C. Hung, C. H. Lee, Y. H. Chen, Y. F. Chen, I. A. Yu, and Y. C. Chen, Highly efficient coherent optical memory based on electromagnetically induced transparency, *Phys. Rev. Lett.* 120(18), 183602 (2018)
76. Y. Wang, J. Li, S. Zhang, K. Su, Y. Zhou, K. Liao, S. Du, H. Yan, and S. L. Zhu, Efficient quantum memory for singlephoton polarization qubits, *Nat. Photonics* 13(5), 346 (2019)
77. D. Schraft, Composite and adiabatic techniques for efficient EIT light storage in Pr^{3+}:Y_2SiO_5, Ph.D. thesis, Technische Universität Darmstadt, 2016
78. G. Heinze, Coherent optical data storage by EIT in a Pr^{3+}:Y_2SiO_5 crystal, Ph. D. thesis, Technische Universität Darmstadt, 2013
79. I. Novikova, A. V. Gorshkov, D. F. Phillips, A. S. Sørensen, M. D. Lukin, and R. L. Walsworth, Optimal control of light pulse storage and retrieval, *Phys. Rev. Lett.* 98(24), 243602 (2007)
80. I. Novikova, N. B. Phillips, and A. V. Gorshkov, Optimal light storage with full pulse-shape control, *Phys. Rev. A* 78(2), 021802 (2008)
81. M. T. Turnbull, P. G. Petrov, C. S. Embrey, A. M. Marino, and V. Boyer, Role of the phase-matching condition in nondegenerate four-wave mixing in hot vapors for the generation of squeezed states of light, *Phys. Rev. A* 88(3), 033845 (2013)
82. V. Boyer, C. F. McCormick, E. Arimondo, and P. D. Lett, Ultraslow propagation of matched pulses by four-wave mixing in an atomic vapor, *Phys. Rev. Lett.* 99(14), 143601 (2007)
83. M. D. Lukin, P. R. Hemmer, M. Löffler, and M. O. Scully, Resonant enhancement of parametric processes via radiative interference and induced coherence, *Phys. Rev. Lett.* 81(13), 2675 (1998)
84. M. Shuker, O. Firstenberg, R. Pugatch, A. Ron, and N. Davidson, Storing images in warm atomic vapor, *Phys. Rev. Lett.* 100(22), 223601 (2008)
85. P. K. Vudyasetu, R. M. Camacho, and J. C. Howell, Storage and retrieval of multimode transverse images in hot atomic rubidium vapor, *Phys. Rev. Lett.* 100(12), 123903 (2008)
86. G. Heinze, A. Rudolf, F. Beil, and T. Halfmann, Storage of images in atomic coherences in a rare-earth-ion-doped solid, *Phys. Rev. A* 81(1), 011401 (2010)
87. G. Heinze, N. Rentzsch, and T. Halfmann, Multiplexed image storage by electromagnetically induced transparency in a solid, *Phys. Rev. A* 86(5), 053837 (2012)
88. L. Ma, X. Lei, J. Yan, R. Li, T. Chai, Z. Yan, X. Jia, C. Xie, and K. Peng, High-performance cavity-enhanced quantum memory with warm atomic cell, *Nat. Commun.* 13(1), 2368 (2022)
89. S. A. Moiseev, and S. Kröll, Complete reconstruction of the quantum state of a single-photon wave packet absorbed by a Doppler-broadened transition, *Phys. Rev. Lett.* 87(17), 173601 (2001)
90. T. W. Mossberg, Time-domain frequency-selective optical data storage, *Opt. Lett.* 7(2), 77 (1982)
91. I. D. Abella, N. A. Kurnit, and S. R. Hartmann, Photon echoes, *Phys. Rev.* 141(1), 391 (1966)
92. E. L. Hahn, Spin echoes, *Phys. Rev.* 80(4), 580 (1950)
93. T. Wang, C. Greiner, J. R. Bochinski, and T. W. Mossberg, Experimental study of photon-echo size in optically thick media, *Phys. Rev. A* 60(2), R757 (1999)
94. C. S. Cornish, W. R. Babbitt, and L. Tsang, Demonstration of highly efficient photon echoes, *Opt. Lett.* 25(17), 1276 (2000)
95. M. Azadeh, C. Sjaarda Cornish, W. R. Babbitt, and L. Tsang, Efficient photon echoes in optically thick media, *Phys. Rev. A* 57(6), 4662 (1998)
96. J. Ruggiero, J. L. Le Gouët, C. Simon, and T. Chanelière, Why the two-pulse photon echo is not a good quantum memory protocol, *Phys. Rev. A* 79(5), 053851 (2009)
97. A. L. Alexander, J. J. Longdell, M. J. Sellars, and N. B. Manson, Photon echoes produced by switching electric

fields, *Phys. Rev. Lett.* 96(4), 043602 (2006)
98. H. de Riedmatten, M. Afzelius, M. U. Staudt, C. Simon, and N. Gisin, A solid-state light–matter interface at the singlephoton level, *Nature* 456(7223), 773 (2008)
99. G. Hétet, J. J. Longdell, M. J. Sellars, P. K. Lam, and B. C. Buchler, Multimodal properties and dynamics of gradient echo quantum memory, *Phys. Rev. Lett.* 101(20), 203601 (2008)
100. S. A. Moiseev, V. F. Tarasov, and B. S. Ham, Quantum memory photon echo-like techniques in solids, *J. Opt. B Quantum Semiclassical Opt.* 5(4), S497 (2003)
101. M. Nilsson and S. Kröll, Solid state quantum memory using complete absorption and re-emission of photons by tailored and externally controlled inhomogeneous absorption profiles, *Opt. Commun.* 247(4–6), 393 (2005)
102. N. Sangouard, C. Simon, M. Afzelius, and N. Gisin, Analysis of a quantum memory for photons based on controlled reversible inhomogeneous broadening, *Phys. Rev. A* 75(3), 032327 (2007)
103. G. Hétet, J. J. Longdell, A. L. Alexander, P. K. Lam, and M. J. Sellars, Electro-optic quantum memory for light using two-level atoms, *Phys. Rev. Lett.* 100(2), 023601 (2008)
104. A. Alexander, J. Longdell, M. Sellars, and N. Manson, Coherent information storage with photon echoes produced by switching electric fields, *J. Lumin.* 127(1), 94 (2007) (Proceedings of the Ninth International Meeting on Hole Burning, Single Molecule, and Related Spectroscopies: Science and Applications)
105. B. Lauritzen, J. Minář, H. de Riedmatten, M. Afzelius, N. Sangouard, C. Simon, and N. Gisin, Telecommunicationwavelength solid-state memory at the single photon level, *Phys. Rev. Lett.* 104(8), 080502 (2010)
106. M. P. Hedges, High performance solid state quantum memory, Ph.D. thesis, The Australian National University, 2011
107. B. Lauritzen, S. R. Hastings-Simon, H. de Riedmatten, M. Afzelius, and N. Gisin, State preparation by optical pumping in erbium-doped solids using stimulated emission and spin mixing, *Phys. Rev. A* 78(4), 043402 (2008)
108. M. P. Hedges, J. J. Longdell, Y. Li, and M. J. Sellars, Efficient quantum memory for light, *Nature* 465(7301), 1052 (2010)
109. F. Grosshans and P. Grangier, Quantum cloning and teleportation criteria for continuous quantum variables, *Phys. Rev. A* 64(1), 010301 (2001)
110. B. M. Sparkes, J. Bernu, M. Hosseini, J. Geng, Q. Glorieux, P. A. Altin, P. K. Lam, N. P. Robins, and B. C. Buchler, Gradient echo memory in an ultra-high optical depth cold atomic ensemble, *New J. Phys.* 15(8), 085027 (2013)
111. Y. W. Cho, G. T. Campbell, J. L. Everett, J. Bernu, D. B. Higginbottom, M. T. Cao, J. Geng, N. P. Robins, P. K. Lam, and B. C. Buchler, Highly efficient optical quantum memory with long coherence time in cold atoms, *Optica* 3(1), 100 (2016)
112. M. Hosseini, B. M. Sparkes, G. Campbell, P. K. Lam, and B. C. Buchler, High efficiency coherent optical memory with warm rubidium vapour, *Nat. Commun.* 2(1), 174 (2011)
113. M. Hosseini, G. Campbell, B. M. Sparkes, P. K. Lam, and B. C. Buchler, Unconditional room-temperature quantum memory, *Nat. Phys.* 7(10), 794 (2011)
114. M. Hosseini, B. M. Sparkes, G. T. Campbell, P. K. Lam, and B. C. Buchler, Storage and manipulation of light using a Raman gradient-echo process, *J. Phys. At. Mol. Opt. Phys.* 45(12), 124004 (2012)
115. G. Hétet, M. Hosseini, B. M. Sparkes, D. Oblak, P. K. Lam, and B. C. Buchler, Photon echoes generated by reversing magnetic field gradients in a rubidium vapor, *Opt. Lett.* 33(20), 2323 (2008)
116. R. L. Ahlefeldt, W. D. Hutchison, N. B. Manson, and M. J. Sellars, Method for assigning satellite lines to crystallographic sites in rare-earth crystals, *Phys. Rev. B* 88(18), 184424 (2013)
117. R. L. Ahlefeldt, D. L. McAuslan, J. J. Longdell, N. B. Manson, and M. J. Sellars, Precision measurement of electronic ion-ion interactions between neighboring Eu^{3+} optical centers, *Phys. Rev. Lett.* 111(24), 240501 (2013)
118. R. L. Ahlefeldt, M. R. Hush, and M. J. Sellars, Ultranarrow optical inhomogeneous linewidth in a stoichiometric rare-earth crystal, *Phys. Rev. Lett.* 117(25), 250504 (2016)
119. A. Ortu, J. V. Rakonjac, A. Holzäpfel, A. Seri, S. Grandi, M. Mazzera, H. de Riedmatten, and M. Afzelius, Multimode capacity of atomic-frequency comb quantum memories, *Quantum Sci. Technol.* 7(3), 035024 (2022)
120. M. R. Hush, C. D. B. Bentley, R. L. Ahlefeldt, M. R. James, M. J. Sellars, and V. Ugrinovskii, Quantum state transfer through time reversal of an optical channel, *Phys. Rev. A* 94(6), 062302 (2016)
121. J. I. Cirac, P. Zoller, H. J. Kimble, and H. Mabuchi, Quantum state transfer and entanglement distribution among distant nodes in a quantum network, *Phys. Rev. Lett.* 78(16), 3221 (1997)
122. M. Afzelius, C. Simon, H. de Riedmatten, and N. Gisin, Multimode quantum memory based on atomic frequency combs, *Phys. Rev. A* 79(5), 052329 (2009)
123. J. Nunn, K. Reim, K. C. Lee, V. O. Lorenz, B. J. Sussman, I. A. Walmsley, and D. Jaksch, Multimode memories in atomic ensembles, *Phys. Rev. Lett.* 101(26), 260502 (2008)
124. I. Usmani, M. Afzelius, H. de Riedmatten, and N. Gisin, Mapping multiple photonic qubits into and out of one solid-state atomic ensemble, *Nat. Commun.* 1(1), 12 (2010)
125. N. Sinclair, E. Saglamyurek, H. Mallahzadeh, J. A. Slater, M. George, R. Ricken, M. P. Hedges, D. Oblak, C. Simon, W. Sohler, and W. Tittel, Spectral multiplexing for scalable quantum photonics using an atomic frequency comb quantum memory and feed-forward control, *Phys. Rev. Lett.* 113(5), 053603 (2014)
126. Z. Q. Zhou, Y. L. Hua, X. Liu, G. Chen, J. S. Xu, Y. J. Han, C. F. Li, and G. C. Guo, Quantum storage of three-dimensional orbital-angular-momentum entanglement in a crystal, *Phys. Rev. Lett.* 115(7), 070502 (2015)
127. B. Lauritzen, J. Minář, H. de Riedmatten, M. Afzelius,

and N. Gisin, Approaches for a quantum memory at telecommunication wavelengths, *Phys. Rev. A* 83(1), 012318 (2011)
128. M. Gündoğan, P. M. Ledingham, A. Almasi, M. Cristiani, and H. de Riedmatten, Quantum storage of a photonic polarization qubit in a solid, *Phys. Rev. Lett.* 108(19), 190504 (2012)
129. Z. Q. Zhou, W. B. Lin, M. Yang, C. F. Li, and G. C. Guo, Realization of reliable solid-state quantum memory for photonic polarization qubit, *Phys. Rev. Lett.* 108(19), 190505 (2012)
130. C. Clausen, F. Bussières, M. Afzelius, and N. Gisin, Quantum storage of heralded polarization qubits in birefringent and anisotropically absorbing materials, *Phys. Rev. Lett.* 108(19), 190503 (2012)
131. C. Laplane, P. Jobez, J. Etesse, N. Timoney, N. Gisin, and M. Afzelius, Multiplexed on-demand storage of polarization qubits in a crystal, *New J. Phys.* 18(1), 013006 (2015)
132. A. Tiranov, P. C. Strassmann, J. Lavoie, N. Brunner, M. Huber, V. B. Verma, S. W. Nam, R. P. Mirin, A. E. Lita, F. Marsili, M. Afzelius, F. Bussières, and N. Gisin, Temporal multimode storage of entangled photon pairs, *Phys. Rev. Lett.* 117(24), 240506 (2016)
133. J. Jin, E. Saglamyurek, M. G. Puigibert, V. Verma, F. Marsili, S. W. Nam, D. Oblak, and W. Tittel, Telecom-wavelength atomic quantum memory in optical fiber for heralded polarization qubits, *Phys. Rev. Lett.* 115(14), 140501 (2015)
134. C. Clausen, I. Usmani, F. Bussières, N. Sangouard, M. Afzelius, H. de Riedmatten, and N. Gisin, Quantum storage of photonic entanglement in a crystal, *Nature* 469(7331), 508 (2011)
135. E. Saglamyurek, N. Sinclair, J. Jin, J. Slater, D. Oblak, F. Bussières, M. George, R. Ricken, W. Sohler, and W. Tittel, Broadband waveguide quantum memory for entangled photons, *Nature* 469(7331), 512 (2011)
136. I. Usmani, C. Clausen, F. Bussières, N. Sangouard, M. Afzelius, and N. Gisin, Heralded quantum entanglement between two crystals, *Nat. Photonics* 6, 234 (2011)
137. J. Rakonjac, G. Corrielli, D. Lago-Rivera, A. Seri, M. Mazzera, S. Grandi, R. Osellame, and H. de Riedmatten, Storage and analysis of light–matter entanglement in a fiber-integrated system, *Sci. Adv.* 8(27), eabn3919 (2022)
138. E. Saglamyurek, J. Jin, V. Verma, M. Shaw, F. Marsili, S. Nam, D. Oblak, and W. Tittel, Quantum storage of entangled telecom-wavelength photons in an erbium-doped optical fibre, *Nat. Photonics* 9(2), 83 (2015)
139. D. Lago-Rivera, S. Grandi, J. Rakonjac, A. Seri, and H. de Riedmatten, Telecom-heralded entanglement between multimode solid-state quantum memories, *Nature* 594(7861), 37 (2021)
140. A. Seri, A. Lenhard, D. Rieländer, M. Gündoğan, P. M. Ledingham, M. Mazzera, and H. de Riedmatten, Quantum correlations between single telecom photons and a multimode ondemand solid-state quantum memory, *Phys. Rev. X* 7(2), 021028 (2017)
141. X. Liu, J. Hu, Z. F. Li, X. Li, P. Y. Li, P. J. Liang, Z. Q. Zhou, C. F. Li, and G. C. Guo, Heralded entanglement distribution between two absorptive quantum memories, *Nature* 594(7861), 41 (2021)
142. D. Lago-Rivera, J. Rakonjac, S. Grandi, and H. Riedmatten, Long-distance multiplexed quantum teleportation from a telecom photon to a solid-state qubit, arXiv: 2209.00802 (2022)
143. J. S. Tang, Z. Q. Zhou, Y. T. Wang, Y. L. Li, X. Liu, Y. L. Hua, Y. Zou, S. Wang, D. Y. He, G. Chen, Y. N. Sun, Y. Yu, M. F. Li, G. W. Zha, H. Q. Ni, Z. C. Niu, C. F. Li, and G. C. Guo, Storage of multiple single-photon pulses emitted from a quantum dot in a solid-state quantum memory, *Nat. Commun.* 6(1), 8652 (2015)
144. N. Gisin and R. Thew, Quantum communication, *Nat. Photonics* 1(3), 165 (2007)
145. F. Bussières, C. Clausen, A. Tiranov, B. Korzh, V. B. Verma, S. W. Nam, F. Marsili, A. Ferrier, P. Goldner, H. Herrmann, C. Silberhorn, W. Sohler, M. Afzelius, and N. Gisin, Quantum teleportation from a telecom-wavelength photon to a solid-state quantum memory, *Nat. Photonics* 8(10), 775 (2014)
146. M. Gündoğan, P. M. Ledingham, K. Kutluer, M. Mazzera, and H. de Riedmatten, Solid state spin-wave quantum memory for time-bin qubits, *Phys. Rev. Lett.* 114(23), 230501 (2015)
147. P. Jobez, N. Timoney, C. Laplane, J. Etesse, A. Ferrier, P. Goldner, N. Gisin, and M. Afzelius, Towards highly multimode optical quantum memory for quantum repeaters, *Phys. Rev. A* 93(3), 032327 (2016)
148. S. Welinski, A. Ferrier, M. Afzelius, and P. Goldner, Highresolution optical spectroscopy and magnetic properties of Yb^{3+} in Y_2SiO_5, *Phys. Rev. B* 94(15), 155116 (2016)
149. A. Ortu, A. Tiranov, S. Welinski, F. Fröwis, N. Gisin, A. Ferrier, P. Goldner, and M. Afzelius, Simultaneous coherence enhancement of optical and microwave transitions in solid-state electronic spins, *Nat. Mater.* 17(8), 671 (2018)
150. T. Böttger, C. W. Thiel, Y. Sun, and R. L. Cone, Optical decoherence and spectral diffusion at 1.5 μm in Er^{3+}:Y_2SiO_5 versus magnetic field, temperature, and Er^{3+} concentration, *Phys. Rev. B* 73(7), 075101 (2006)
151. M. Businger, L. Nicolas, T. S. Mejia, A. Ferrier, P. Goldner, and M. Afzelius, Non-classical correlations over 1250 modes between telecom photons and 979-nm photons stored in $171Yb^{3+}$:Y_2SiO_5, *Nat. Commun.* 13(1), 6438 (2022)
152. E. Saglamyurek, M. Grimau Puigibert, Q. Zhou, L. Giner, F. Marsili, V. B. Verma, S. Woo Nam, L. Oesterling, D. Nippa, D. Oblak, and W. Tittel, A multiplexed light-matter interface for fibre-based quantum networks, *Nat. Commun.* 7(1), 11202 (2016)
153. A. Seri, D. Lago-Rivera, A. Lenhard, G. Corrielli, R. Osellame, M. Mazzera, and H. de Riedmatten, Quantum storage of frequency-multiplexed heralded single photons, *Phys. Rev. Lett.* 123(8), 080502 (2019)
154. S. H. Wei, B. Jing, X. Y. Zhang, J. Y. Liao, H. Li, L. X. You, Z. Wang, Y. Wang, G. W. Deng, H. Z. Song, D. Oblak, G. C. Guo, and Q. Zhou, Storage of 1650 modes of single photons at telecom wavelength, arXiv: 2209.00802 (2022)

155. M. Sabooni, Q. Li, S. Kröll, and L. Rippe, Efficient quantum memory using a weakly absorbing sample, *Phys. Rev. Lett.* 110(13), 133604 (2013)
156. Y. Ma, Y. Z. Ma, Z. Q. Zhou, C. F. Li, and G. C. Guo, One hour coherent optical storage in an atomic frequency comb memory, *Nat. Commun.* 12(1), 2381 (2021)
157. A. Ortu, A. Holzäpfel, J. Etesse, and M. Afzelius, Storage of photonic time-bin qubits for up to 20 ms in a rare-earth doped crystal, *npj Quantum Inform.* 8, 29 (2022)
158. B. Kraus, W. Tittel, N. Gisin, M. Nilsson, S. Kröll, and J. I. Cirac, Quantum memory for nonstationary light fields based on controlled reversible inhomogeneous broadening, *Phys. Rev. A* 73(2), 020302 (2006)
159. S. A. Moiseev, S. N. Andrianov, and F. F. Gubaidullin, Efficient multimode quantum memory based on photon echo in an optimal QED cavity, *Phys. Rev. A* 82(2), 022311 (2010)
160. M. Afzelius and C. Simon, Impedance-matched cavity quantum memory, *Phys. Rev. A* 82(2), 022310 (2010)
161. P. Jobez, I. Usmani, N. Timoney, C. Laplane, N. Gisin, and M. Afzelius, Cavity-enhanced storage in an optical spin-wave memory, *New J. Phys.* 16(8), 083005 (2014)
162. J. H. Davidson, P. Lefebvre, J. Zhang, D. Oblak, and W. Tittel, Improved light-matter interaction for storage of quantum states of light in a thulium-doped crystal cavity, *Phys. Rev. A* 101(4), 042333 (2020)
163. S. Duranti, Highly efficient qubit storage in an atomic frequency comb based quantum memory, in: Rare Earth Ions for Quantum Information Workshop, 2022
164. M. Afzelius, I. Usmani, A. Amari, B. Lauritzen, A. Walther, C. Simon, N. Sangouard, J. Minář, H. de Riedmatten, N. Gisin, and S. Kröll, Demonstration of atomic frequency comb memory for light with spin-wave storage, *Phys. Rev. Lett.* 104(4), 040503 (2010)
165. L. Rippe, M. Nilsson, S. Kröll, R. Klieber, and D. Suter, Experimental demonstration of efficient and selective population transfer and qubit distillation in a rare-earth-metal-ion-doped crystal, *Phys. Rev. A* 71(6), 062328 (2005)
166. M. S. Silver, R. I. Joseph, and D. I. Hoult, Selective spin inversion in nuclear magnetic resonance and coherent optics through an exact solution of the Bloch-Riccati equation, *Phys. Rev. A* 31(4), 2753 (1985)
167. M. Tian, T. Chang, K. D. Merkel, and W. Randall, Reconfiguration of spectral absorption features using a frequency-chirped laser pulse, *Appl. Opt.* 50(36), 6548 (2011)
168. M. Businger, A. Tiranov, K. T. Kaczmarek, S. Welinski, Z. Zhang, A. Ferrier, P. Goldner, and M. Afzelius, Optical spin-wave storage in a solid-state hybridized electron-nuclear spin ensemble, *Phys. Rev. Lett.* 124(5), 053606 (2020)
169. S. E. Beavan, P. M. Ledingham, J. J. Longdell, and M. J. Sellars, Photon echo without a free induction decay in a double-λ system, *Opt. Lett.* 36(7), 1272 (2011)
170. Y. Z. Ma, M. Jin, D. L. Chen, Z. Q. Zhou, C. F. Li, and G. C. Guo, Elimination of noise in optically rephased photon echoes, *Nat. Commun.* 12(1), 4378 (2021)
171. J. V. Rakonjac, Y. H. Chen, S. P. Horvath, and J. J. Longdell, Long spin coherence times in the ground state and in an optically excited state of $167Er^{3+}$: Y_2SiO_5 at zero magnetic field, *Phys. Rev. B* 101(18), 184430 (2020)
172. M. Rančić, M. P. Hedges, R. L. Ahlefeldt, and M. J. Sellars, Coherence time of over a second in a telecom-compatible quantum memory storage material, *Nat. Phys.* 14(1), 50 (2018)
173. M. Zhong, Development of persistent quantum memories, Ph. D. thesis, The Australian National University, 2017
174. V. Damon, M. Bonarota, A. Louchet-Chauvet, T. Chanelière, and J. L. L. Gouët, Revival of silenced echo and quantum memory for light, *New J. Phys.* 13(9), 093031 (2011)
175. M. Bonarota, J. Dajczgewand, A. Louchet-Chauvet, J. L. L. Gouët, and T. Chanelière, Photon echo with a few photons in two-level atoms, *Laser Phys.* 24(9), 094003 (2014)
176. C. Liu, Z. Q. Zhou, T. X. Zhu, L. Zheng, M. Jin, X. Liu, P. Y. Li, J. Y. Huang, Y. Ma, T. Tu, T. S. Yang, C. F. Li, and G. C. Guo, Reliable coherent optical memory based on a laser-written waveguide, *Optica* 7(2), 192 (2020)
177. J. Dajczgewand, J. L. L. Gouët, A. Louchet-Chauvet, and T. Chanelière, Large efficiency at telecom wavelength for optical quantum memories, *Opt. Lett.* 39(9), 2711 (2014)
178. M. Jin, Y. Z. Ma, Z. Q. Zhou, C. F. Li, and G. C. Guo, A faithful solid-state spin-wave quantum memory for polarization qubits, *Sci. Bull. (Beijing)* 67(7), 676 (2022)
179. Z. Q. Zhou, A spin-wave integrated quantum memory, in: Rare Earth Ions for Quantum Information Workshop, 2022
180. S. P. Horvath, M. K. Alqedra, A. Kinos, A. Walther, J. M. Dahlström, S. Kröll, and L. Rippe, Noise-free on-demand atomic frequency comb quantum memory, *Phys. Rev. Res.* 3(2), 023099 (2021)
181. T. X. Zhu, C. Liu, M. Jin, M. X. Su, Y. P. Liu, W. J. Li, Y. Ye, Z. Q. Zhou, C. F. Li, and G. C. Guo, On-demand integrated quantum memory for polarization qubits, *Phys. Rev. Lett.* 128(18), 180501 (2022)
182. C. Liu, T. X. Zhu, M. X. Su, Y. Z. Ma, Z. Q. Zhou, C. F. Li, and G. C. Guo, On-demand quantum storage of photonic qubits in an on-chip waveguide, *Phys. Rev. Lett.* 125(26), 260504 (2020)
183. I. Craiciu, M. Lei, J. Rochman, J. G. Bartholomew, and A. Faraon, Multifunctional on-chip storage at telecommunication wavelength for quantum networks, *Optica* 8(1), 114 (2021)
184. A. Tiranov, J. Lavoie, A. Ferrier, P. Goldner, V. B. Verma, S. W. Nam, R. P. Mirin, A. E. Lita, F. Marsili, H. Herrmann, C. Silberhorn, N. Gisin, M. Afzelius, and F. Bussières, Storage of hyperentanglement in a solid-state quantum memory, *Optica* 2(4), 279 (2015)
185. C. Simon and J. W. Pan, Polarization entanglement purification using spatial entanglement, *Phys. Rev. Lett.* 89(25), 257901 (2002)
186. S. Ecker, F. Bouchard, L. Bulla, F. Brandt, O. Kohout, F. Steinlechner, R. Fickler, M. Malik, Y. Guryanova,

R. Ursin, and M. Huber, Overcoming noise in entanglement distribution, *Phys. Rev. X* 9(4), 041042 (2019)
187. L. Sheridan and V. Scarani, Security proof for quantum key distribution using qudit systems, *Phys. Rev. A* 82(3), 030301 (2010)
188. K. R. Ferguson, Generation and storage of optical entanglement in a solid state spin-wave quantum memory, Ph. D. thesis, The Australian National University, 2016
189. S. E. Beavan, Photon-echo rephasing of spontaneous emission from an ensemble of rare-earth ions, Ph. D. thesis, The Australian National University, 2012
190. P. M. Ledingham, W. R. Naylor, J. J. Longdell, S. E. Beavan, and M. J. Sellars, Nonclassical photon streams using rephased amplified spontaneous emission, *Phys. Rev. A* 81(1), 012301 (2010)
191. P. M. Ledingham, W. R. Naylor, and J. J. Longdell, Experimental realization of light with time-separated correlations by rephasing amplified spontaneous emission, *Phys. Rev. Lett.* 109(9), 093602 (2012)
192. S. E. Beavan, M. P. Hedges, and M. J. Sellars, Demonstration of photon-echo rephasing of spontaneous emission, *Phys. Rev. Lett.* 109(9), 093603 (2012)
193. K. R. Ferguson, S. E. Beavan, J. J. Longdell, and M. J. Sellars, Generation of light with multimode time-delayed entanglement using storage in a solid-state spin-wave quantum memory, *Phys. Rev. Lett.* 117(2), 020501 (2016)
194. C. Laplane, P. Jobez, J. Etesse, N. Gisin, and M. Afzelius, Multimode and long-lived quantum correlations between photons and spins in a crystal, *Phys. Rev. Lett.* 118(21), 210501 (2017)
195. K. Kutluer, M. Mazzera, and H. de Riedmatten, Solid-state source of nonclassical photon pairs with embedded multimode quantum memory, *Phys. Rev. Lett.* 118(21), 210502 (2017)
196. K. Kutluer, E. Distante, B. Casabone, S. Duranti, M. Mazzera, and H. de Riedmatten, Time entanglement between a photon and a spin wave in a multimode solid-state quantum memory, *Phys. Rev. Lett.* 123(3), 030501 (2019)
197. P. Sekatski, N. Sangouard, N. Gisin, H. de Riedmatten, and M. Afzelius, Photon-pair source with controllable delay based on shaped inhomogeneous broadening of rare-earth-metal-doped solids, *Phys. Rev. A* 83(5), 053840 (2011)
198. C. Ottaviani, C. Simon, H. de Riedmatten, M. Afzelius, B. Lauritzen, N. Sangouard, and N. Gisin, Creating single collective atomic excitations via spontaneous Raman emission in inhomogeneously broadened systems: Beyond the adiabatic approximation, *Phys. Rev. A* 79(6), 063828 (2009)
199. L. Béguin, J. P. Jahn, J. Wolters, M. Reindl, Y. Huo, R. Trotta, A. Rastelli, F. Ding, O. G. Schmidt, P. Treutlein, and R. J. Warburton, On-demand semiconductor source of 780-nm single photons with controlled temporal wave packets, *Phys. Rev. B* 97(20), 205304 (2018)
200. A. J. Bennett, J. P. Lee, D. J. P. Ellis, T. Meany, E. Murray, F. F. Floether, J. P. Griffths, I. Farrer, D. A. Ritchie, and A. J. Shields, Cavity-enhanced coherent light scattering from a quantum dot, *Sci. Adv.* 2(4), e1501256 (2016)
201. T. M. Sweeney, S. G. Carter, A. S. Bracker, M. Kim, C. S. Kim, L. Yang, P. M. Vora, P. G. Brereton, E. R. Cleveland, and D. Gammon, Cavity-stimulated Raman emission from a single quantum dot spin, *Nat. Photonics* 8(6), 442 (2014)
202. X. Y. Zhang, B. Jing, B. Zhang, H. Li, S. H. Wei, C. Li, J. Y. Liao, G. W. Deng, Y. Wang, H. Z. Song, L. X. You, F. Chen, G. C. Guo, and Q. Zhou, Storage of 147 temporal modes of telecom-band single photon with fiber-pigtailed Er^{3+}: Linbo3 waveguide, in: Conference on Lasers and Electro-Optics, Optica Publishing Group, 2022, p. JTh6A. 9
203. I. Craiciu, M. Lei, J. Rochman, J. M. Kindem, J. G. Bartholomew, E. Miyazono, T. Zhong, N. Sinclair, and A. Faraon, Nanophotonic quantum storage at telecommunication wavelength, *Phys. Rev. Appl.* 12(2), 024062 (2019)
204. T. Zhong, J. M. Kindem, J. G. Bartholomew, J. Rochman, I. Craiciu, E. Miyazono, M. Bettinelli, E. Cavalli, V. Verma, S. W. Nam, F. Marsili, M. D. Shaw, A. D. Beyer, and A. Faraon, Nanophotonic rare-earth quantum memory with optically controlled retrieval, *Science* 357(6358), 1392 (2017)
205. T. Zhong and P. Goldner, Emerging rare-earth doped material platforms for quantum nanophotonics, *Nanophotonics* 8(11), 2003 (2019)
206. A. Fossati, S. Liu, J. Karlsson, A. Ikesue, A. Tallaire, A. Ferrier, D. Serrano, and P. Goldner, A frequency-multiplexed coherent electro-optic memory in rare earth doped nanoparticles, *Nano Lett.* 20, 7087 (2020)
207. M. F. Askarani, M. G. Puigibert, T. Lutz, V. B. Verma, M. D. Shaw, S. W. Nam, N. Sinclair, D. Oblak, and W. Tittel, Storage and reemission of heralded telecommunication-wavelength photons using a crystal waveguide, *Phys. Rev. Appl.* 11(5), 054056 (2019)
208. R. Valivarthi, S. I. Davis, C. Peña, S. Xie, N. Lauk, L. Narváez, J. P. Allmaras, A. D. Beyer, Y. Gim, M. Hussein, G. Iskander, H. L. Kim, B. Korzh, A. Mueller, M. Rominsky, M. Shaw, D. Tang, E. E. Wollman, C. Simon, P. Spentzouris, D. Oblak, N. Sinclair, and M. Spiropulu, Teleportation systems toward a quantum internet, *PRX Quantum* 1(2), 020317 (2020)
209. E. Miyazono, T. Zhong, I. Craiciu, J. M. Kindem, and A. Faraon, Coupling of erbium dopants to yttrium orthosilicate photonic crystal cavities for on-chip optical quantum memories, *Appl. Phys. Lett.* 108(1), 011111 (2016)